Journal of
Mechanics of
Materials and Structures

A UNIFIED THEORY FOR CONSTITUTIVE MODELING OF COMPOSITES

Wenbin Yu

Volume 11, No. 4 July 2016

msp

JOURNAL OF MECHANICS OF MATERIALS AND STRUCTURES
Vol. 11, No. 4, 2016
dx.doi.org/10.2140/jomms.2016.11.379

A UNIFIED THEORY FOR CONSTITUTIVE MODELING OF COMPOSITES

WENBIN YU

A unified theory for multiscale constitutive modeling of composites is developed using the concept of structure genomes. Generalized from the concept of the representative volume element, a structure genome is defined as the smallest mathematical building block of a structure. Structure genome mechanics governs the necessary information to bridge the microstructure length scale of composites and the macroscopic length scale of structural analysis and provides a unified theory to construct constitutive models for structures including three-dimensional structures, beams, plates, and shells over multiple length scales. For illustration, this paper is restricted to construct the Euler–Bernoulli beam model, the Kirchhoff–Love plate/shell model, and the Cauchy continuum model for structures made of linear elastic materials. Geometrical nonlinearity is systematically captured for beams, plates/shells, and Cauchy continuum using a unified formulation. A general-purpose computer code called SwiftComp (accessible at https://cdmhub.org/resources/scstandard) implements this unified theory and is used in a few example cases to demonstrate its application.

1. Introduction

Structural analyses are often carried out using finite element analysis (FEA) in terms of three-dimensional (3D) solid elements, two-dimensional (2D) plate or shell elements or one-dimensional (1D) beam elements (see Figure 1). Here, the notation of 1D, 2D, or 3D refers to the number of coordinates needed to describe the analysis domain. It is not related with the dimensionality of the behavior. For example, a beam element can have three-dimensional behavior as it can deform in three directions. A constitutive relation is needed for the corresponding structural element. For isotropic homogeneous structures, material properties such as Young's modulus and Poisson's ratio are direct inputs for structural analysis using solid elements; these properties, combined with the geometry of the structure, can be used for plate/shell/beam elements. However, such straightforwardness does not exist for composite structures featuring anisotropy and/or heterogeneity. Consider a typical composite rotor blade of length 8.6 m and chord 0.72 m, with a main D-spar composed of 60 graphite/epoxy plies each with a ply thickness of 125 μm. To directly use the properties of graphite/epoxy composite plies in the blade analysis, at least one 3D solid element through the ply thickness should be used. Sometimes several layers are commonly lumped together into a single element with "smeared properties", however, this will result in approximate solutions that would negate the supposed accuracy advantage gained by the use of 3D solid elements. Suppose one uses 20-noded brick elements with a 1:10 thickness-length ratio: it is estimated that around ten billion degrees of freedom are needed for the blade analysis. Such a huge FEA model is too costly for effective blade design and analysis. An alternative is to model rotor blades as beams [Yu et al. 2012]

Keywords: Mechanics of Structure Genome, Structural Mechanics, Micromechanics, Composites Mechanics, Homogenization.

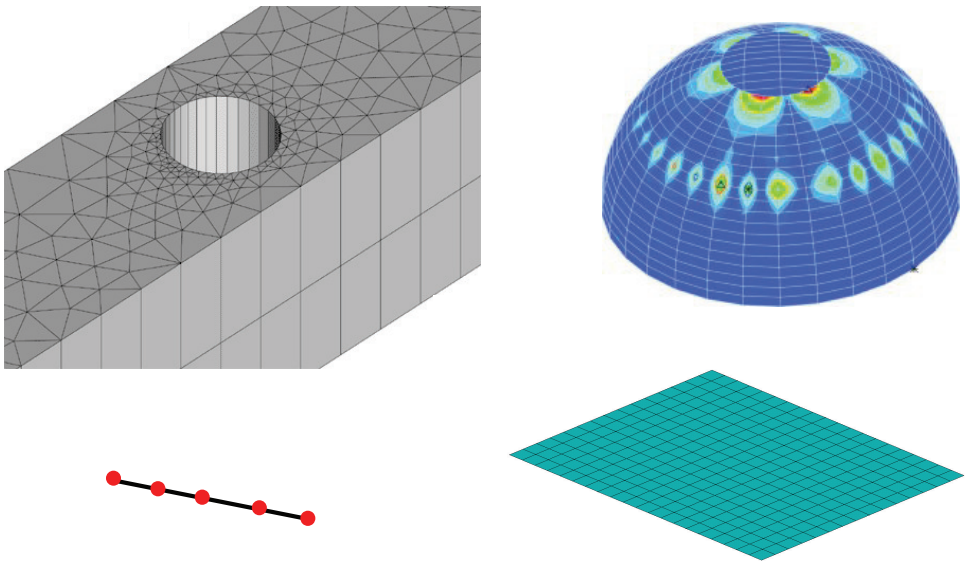

Figure 1. Typical structural elements: a) 3D solid elements; b) 2D shell elements; c) 1D beam elements; d) 2D plate elements.

with models to bridge the material properties of composite plies and the beam properties, and compute the stress fields within each layer for failure and safety predictions.

Sometimes, it is desirable to start the modeling process of composite structures from the fiber (usually the size of a few microns) and the matrix. A multiscale modeling approach is needed to link micromechanics [Li and Wang 2008; Nemat-Nasser and Hori 1998; Aboudi et al. 2012; Fish 2013] and structural mechanics [Reddy 2004; Kollár and Springer 2009; Carrera et al. 2014]. Many micromechanics models have been introduced to provide either rigorous bounds, such as the rules of mixtures [Hill 1952], Hashin–Shtrikman bounds [Hashin and Shtrikman 1962], third-order bounds [Milton 2002], and higher-order bounds [Torquato 2002]; or approximate predictions such as Mori–Tanaka method [Mori and Tanaka 1973], the method of cells [Aboudi 1982; 1989] and its variants [Paley and Aboudi 1992; Aboudi et al. 2001; 2012; Williams 2005], mathematical homogenization theories [Bensoussan et al. 1978; Murakami and Toledano 1990; Guedes and Kikuchi 1990; Michel et al. 1999; Fish 2013; Zhang and Oskay 2016], finite element approaches using conventional stress analysis of representative volume elements (RVEs) [Sun and Vaidya 1996; Berger et al. 2006], Voronoi cell finite element method [Ghosh 2011], and variational asymptotic method for unit cell homogenization [Yu and Tang 2007; Zhang and Yu 2014]. Even more structural models have been developed for composite structures which are usually based on a set of *a priori* assumptions. For composite laminates, the displacement field is usually assumed to be expressed in terms of 2D functions with known distributions through the thickness [Reddy 2004; Khandan et al. 2012]. For example, the classical laminated plate theory (CLPT) was derived based on the assumption that the transverse normal remains normal to the reference surface and is rigid. The first-order shear-deformation theory was derived based on the assumption that the transverse normal remains straight and rigid, but does not necessarily remain normal. Many assumptions have been proposed in the literature including equivalent single-layer assumptions [Reddy 1984; Mantari et al. 2012], layerwise assumptions

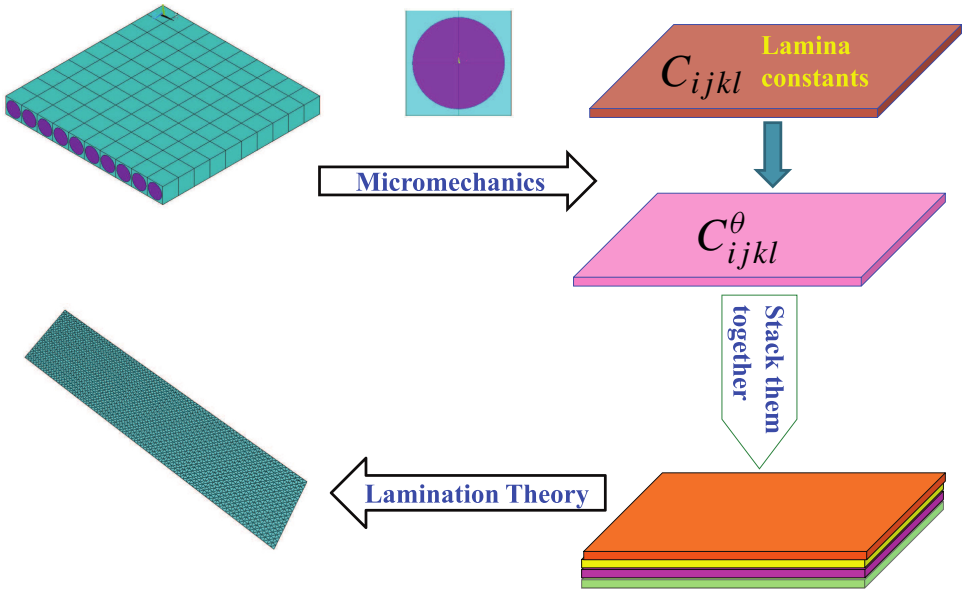

Figure 2. Traditional multiscale modeling approach illustrated for composite laminates.

[Plagianakos and Saravanos 2009; Icardi and Ferrero 2010], and zigzag assumptions [Carrera 2003; Xiaohui et al. 2011]. Recently, Carrera [2012] developed a unified formulation to systematically construct all these models based on *a priori* assumptions [Demasi and Yu 2012]. To avoid these assumptions, asymptotic models were developed [Maugin and Attou 1990; Cheng and Batra 2000; Kalamkarov and Kolpakov 2001; Reddy and Cheng 2001; Kalamkarov et al. 2009; Kim 2009; Skoptsov and Sheshenin 2011] with the field variables expressed using a formal asymptotic series.

Common multiscale modeling approaches usually apply a two-step approach (TSA), which carry out a micromechanical analysis followed by a structural analysis. For example, for composite laminates, a micromechanics model is first used to compute the lamina constants in terms of the microstructure — commonly called the RVE or unit cell (UC) — of the composite ply, then a lamination theory is used to construct a structural model for the macroscopic analysis (see Figure 2). There are three possible issues with this approach. First, the microstructural scale is implicitly assumed to be much smaller than the structural scale which might cause significant error for structures where one of the dimensions is similar in size to the microstructure, such as thin laminates or sandwich structures with a thick core. Second, as shown in Figure 3, TSA creates artificial discontinuities at the layer interfaces because the original heterogeneous panel (Figure 3a) is effectively replaced with an imaginary panel made of homogeneous layers (Figure 3b). The real discontinuities happen at the interfaces between the fiber and matrix if perfect bonding is assumed between layers, which is normally done in lamination theories. Third, composite damage might initiate and propagate in such a way that the separation of microscale and laminate scale in TSA is not valid any more. These issues have been noticed by Pagano and Rybicki [1974]. The focus of this paper is to potentially resolve these issues by developing a unified theory to link the lowest scale of interest to the structural scale.

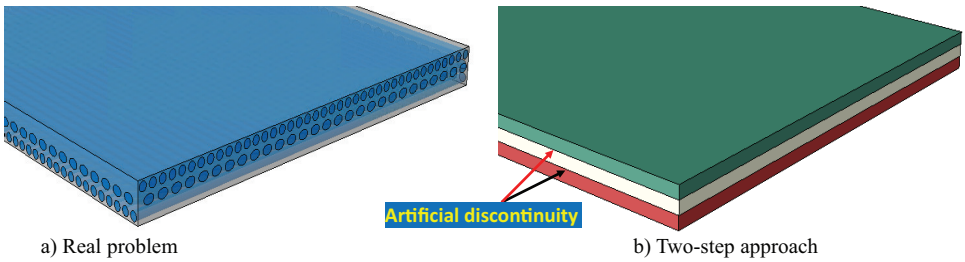

Figure 3. Artificial discontinuity created by the lamination theory.

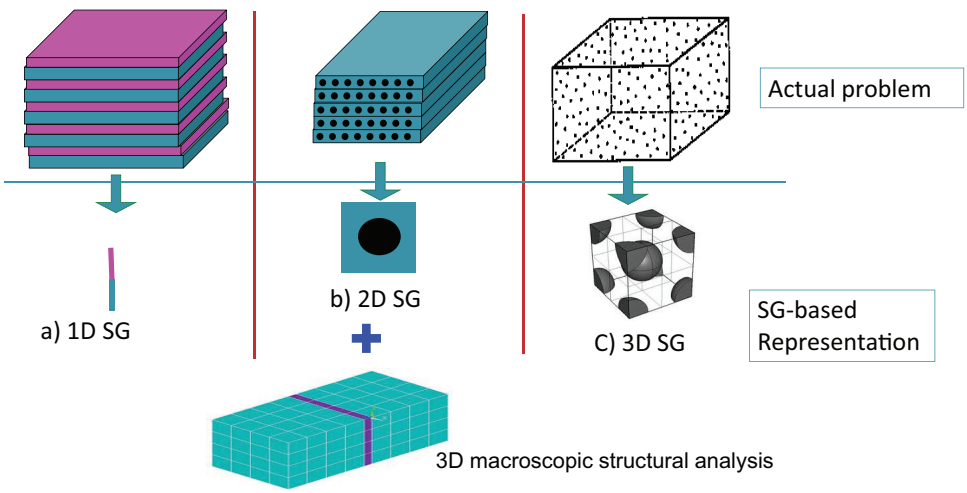

Figure 4. Analysis of 3D heterogeneous structures approximated by a constitutive modeling over SG and a corresponding 3D macroscopic structural analysis.

2. Structure Genome (SG)

A genome serves as a blueprint for an organism's growth and development. We can extrapolate this word into nonbiological contexts to connote a *fundamental building block* of a system. A new concept called the Structure Genome (SG) is defined as the *smallest mathematical building block* of the structure, to emphasize the fact that it contains all the constitutive information needed for a structure in the same fashion that the genome contains all the genetic information for an organism's growth and development. It is noted that this work uses the continuum hypothesis, and scales below the continuum scale (such as the atomic scale) are not considered here.

2.1. ***SG for 3D structures.*** As shown in Figure 4, analyses of 3D heterogeneous structures can be approximated by a 3D macroscopic structural analysis with the material properties provided by a constitutive modeling of a SG. For 3D structures, the SG serves a similar role as the RVE in micromechanics. However, they are significantly different, so the new term (SG) is used to avoid confusion. For example, for a structure made of composites featuring 1D heterogeneity (e.g. binary composites made of two alternating layers, Figure 4a), the SG will be a straight line with two segments denoting corresponding phases. One

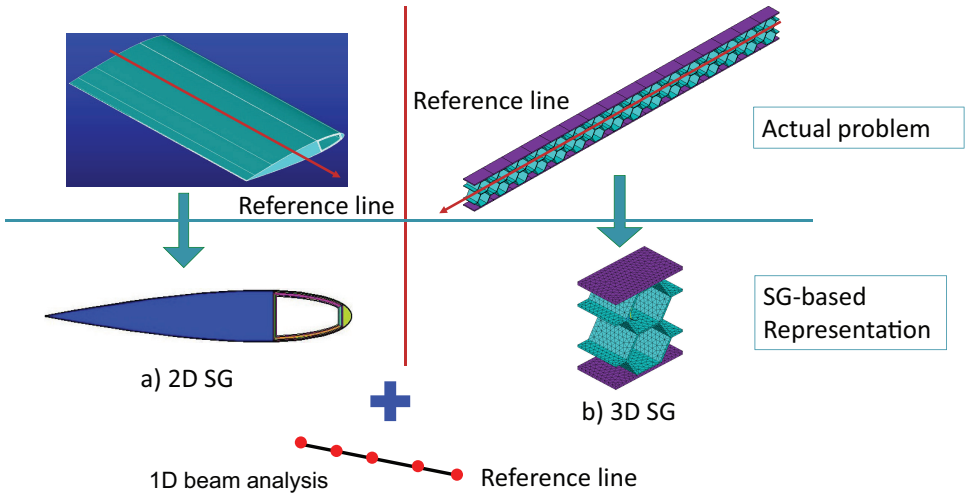

Figure 5. Analysis of beam-like structures approximated by a constitutive modeling over SG and a corresponding 1D beam analysis.

can mathematically repeat this line in-plane to build the two layers of the binary composite, and then repeat the binary composite out of plane to build the entire structure. Another possible application is to model a laminate as an equivalent homogeneous solid. The transverse normal line is the 1D SG for the laminate. The constitutive modeling over the 1D SG can compute the complete set of 3D properties and local fields. Such applications of the SG are not equivalent to the RVE. For a structure made of composites featuring 2D heterogeneity (e.g. continuous unidirectional fiber reinforced composites, Figure 4b), the SG will be 2D. Although 2D RVEs are also used in micromechanics, only in-plane properties and local fields can be obtained from common RVE-based models. If the complete set of properties are needed for a 3D structural analysis, a 3D RVE is usually required [Sun and Vaidya 1996; Fish 2013], while a 2D domain is sufficient if it is modeled using SG-based models (Figure 4b) or some semianalytical models such as GMC/HFGMC [Aboudi et al. 2012]. For a structure made of composites featuring 3D heterogeneity (e.g. particle reinforced composites, Figure 4c), the SG will be a 3D volume. Although a 3D SG for 3D structures represents the most similar case to a RVE, indispensable boundary conditions in terms of displacements and tractions in RVE-based models are not needed for SG-based models.

2.2. ***SG for beams/plates/shells.*** SG allows the connection of microstructure studies with beam/plate/shell analyses. For example, the structural analysis of slender (beam-like) structures can use beam elements (Figure 5). If the beam has uniform cross-sections which could be made of homogeneous materials or composites (Figure 5a), its SG is the 2D cross-sectional domain because the cross-section can be projected along the beam reference line to form the beam-like structure. This inspires a *new perspective* toward beam modeling [Yu et al. 2012], a traditional branch of structural mechanics. If the beam reference line is considered as a 1D continuum, every material point of this continuum has a cross-section as its microstructure. In other words, *constitutive modeling for beams can be effectively viewed as an application of micromechanics.* If the beam is also heterogeneous in the spanwise direction (Figure 5b), a 3D SG is needed to describe the microstructure of the 1D continuum, the behavior of which is governed

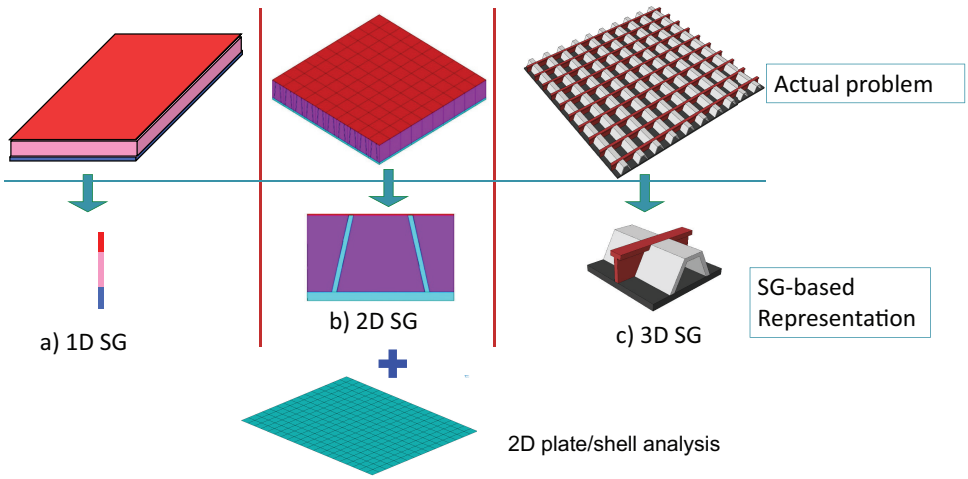

Figure 6. Analysis of plate-like structures approximated by a constitutive modeling over SG and a corresponding 2D plate analysis.

by the 1D beam analysis. Note that SG is different from the traditional notion of obtaining apparent material properties for a structure. For example, the flexural stiffness of an I-beam could be given by E^*I, such that an I-beam could be represented by a rectangular beam but with an apparent Young's modulus E^* so that $E^*I = E^* \times bd^3/12$ with b as the width and d as the height. Instead, using SG we can obtain the bending stiffness directly for the I-beam without referring to a geometry factor (reinterpreting it as a rectangular beam). No intermediate step such as E^* is needed. The concept of SG provides a unified treatment of structural modeling and micromechanics modeling and enables us to collapse the cross-section or a 3D beam segment into a material point for a beam analysis over the reference line with a possible, fully populated 4×4 stiffness matrix simultaneously accounting for extension, torsion, and bending in two directions.

If the structural analysis uses plate/shell elements, a SG can also be chosen properly. For illustrative purposes, typical SGs of plate-like structures are sketched in Figure 6. If the plate-like structures feature no in-plane heterogeneities (Figure 6a), the SG is the transverse normal line with each segment denoting the corresponding layer. For a sandwich panel with a core corrugated in one direction (Figure 6b), the SG is 2D. If the panel is heterogeneous in both in-plane directions (Figure 6c), such as a stiffened panel with stiffeners running in both directions, the SG is 3D. Despite the different dimensionalities of the SGs, the constitutive modeling should output structural properties for the corresponding structural analysis (such as the A, B, and D matrices for the Kirchhoff–Love plate model) and relations to express the original 3D fields in terms of the global behavior (e.g., moments, curvatures, etc.) obtained from the plate/shell analysis. It is known that theories of plates/shells traditionally belong to structural mechanics, but the constitutive modeling of these structures can be treated as special micromechanics applications using the SG concept. For a plate/shell-like structure, if the reference surface is considered as a 2D continuum, every material point of this continuum has an associated SG as its microstructure.

It is easy to identify SGs for periodic structures as shown in Figures 4, 5, and 6. For structures which are not globally periodic, we usually assume that the structure is at least periodic in the neighborhood of

a material point in the macroscopic structural analysis, the so-called local periodicity assumption implicit in all multiscale modeling approaches [Fish 2013]. For nonlinear behavior, it is also possible that the smallest mathematical building block of the structure is not sufficient as the characteristic length scale of the nonlinear behavior may cover several building blocks. For this case, SG should be interpreted as the smallest mathematical building block necessary to represent the nonlinear behavior.

SG serves as the link between the original structure with microscopic details and the macroscopic structural analysis. Here, the terms "microstructure" and "microscopic details" are used in a general sense: any details explicitly existing in a SG but not in the macroscopic structural analysis are termed microscopic details in this paper. Here and later in the paper, the real structure with microscopic details is termed as the original structure and the structure used in the macroscopic structural analysis is termed as the macroscopic structural model. It is also interesting to point out the relation between the SG concept and the idea of substructuring or superelement, which is commonly used in sizing software such as HyperSizer [Collier et al. 2002]. A line element in the global analysis could correspond to a box beam made of four laminated walls, and a surface element could correspond to a sandwich panel with laminated face sheets and a corrugated core. For these cases, SG and its companion mechanics presented below provide a rigorous and systematic approach based on micromechanics to compute the constitutive models for the line and surface elements and the local fields within the original structures.

3. Mechanics of structure genome (MSG)

SG serves as the fundamental building block of a structure; whether it is a 3D structure or a beam, plate, or shell. For SG to not merely remain as a concept, it must be governed by a physics-based theory, namely mechanics of structure genome (MSG), so that there is a two-way communication between microstructural details and structural analysis: microstructural information can be rigorously passed to structural analysis to predict structural performance, and structural performance can be passed back to predict the local fields within the microstructure for failure prediction and other detailed analyses.

A structural model contains kinematics, kinetics, and constitutive relations. On the one hand, kinematics deals with strain-displacement relations and compatibility equations, while on the other hand, kinetics deals with stress and equations of motion. Constitutive relations relate stress and strain. Both kinematics and kinetics can be formulated exactly within the framework of continuum mechanics and remain the same for the same structural model independent of the composition of the structure. Constitutive relations are where the difference comes from and are ultimately approximate because a hypothetical continuum is used to model the underlying atomic structure. Some criteria is needed for us to minimize the loss of information between the original model describing the microscopic details and the model used for the macroscopic structural analysis. For elastic materials, this can be achieved by minimizing the difference between the strain energy of the materials stored in SG and that stored in the macroscopic structural model.

3.1. ***Kinematics.*** The first step in formulating MSG is to express the kinematics, including the displacement field and the strain field, of the original structures in terms of those in the macroscopic structural model. Although the SG concept is applicable to original structures made of materials admitting general continuum descriptions such as the Cosserat continuum [Cosserat and Cosserat 1909], this work focuses on materials admitting the Cauchy continuum description.

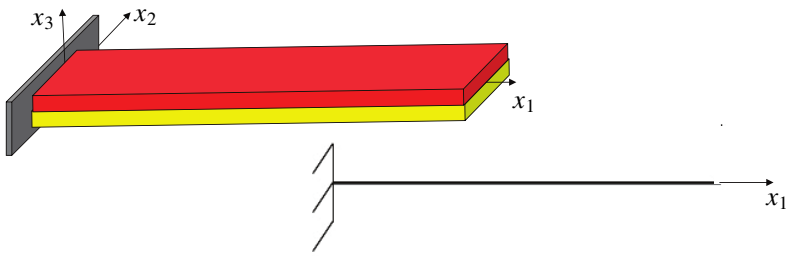

Figure 7. Macrocoordinates (x_1, x_2, x_3) and eliminated coordinates (x_2, x_3) of a beam.

3.1.1. *Coordinate systems.* Let us use x_i, called macrocoordinates here, to denote the coordinates describing the original structure. The coordinates could be general curvilinear coordinates. However, without loss of generality, we choose an orthogonal system of arc-length coordinates. If the structure is dimensionally reducible, some of the macrocoordinates x_α, called eliminated coordinates here, correspond to the dimensions eliminated in the macroscopic structural model. Here and throughout the paper, Greek indices assume values corresponding to the eliminated macrocoordinates, Latin indices k, l, m assume values corresponding to the macrocoordinates remaining in the macroscopic structural model, and other Latin indices assume 1, 2, 3. Repeated indices are summed over their range except where explicitly indicated.

For beam-like structures, only x_1, describing the beam reference line, will remain in the final beam model, while x_2, x_3, the cross-sectional coordinates, will be eliminated (see Figure 7); for plate/shell-like structures, x_1 and x_2, describing the plate/shell reference surface, will remain in the final plate/shell model, while x_3, the thickness coordinate, will be eliminated. For this reason, the beam model is called a 1D continuum model because all the unknown fields are functions of x_1 only. Similarly, the plate/shell model is called a 2D continuum model because all the unknown fields are functions of x_1 and x_2 only.

Since the size of a SG is much smaller than the wavelength of the macroscopic deformation, we introduce microcoordinates $y_i = x_i/\varepsilon$ to describe the SG, with ε being a small parameter. This basically enables a zoom-in view of the SG at a size similar to the macroscopic structure. If the SG is 1D, only y_3 is needed; if the SG is 2D, y_2 and y_3 are needed; if the SG is 3D, all three coordinates y_1, y_2, y_3 are needed. In multiscale structural modeling, a field function of the original structure can be generally written as a function of the macrocoordinates x_k which remain in the macroscopic structural model and the microcoordinates y_j. Following [Bensoussan et al. 1978], the partial derivative of a function $f(x_k, y_j)$ can be expressed as

$$\frac{\partial f(x_k, y_j)}{\partial x_i} = \frac{\partial f(x_k, y_j)}{\partial x_i}\bigg|_{y_j=\text{const}} + \frac{1}{\varepsilon}\frac{\partial f(x_k, y_j)}{\partial y_i}\bigg|_{x_k=\text{const}} \equiv f_{,i} + \frac{1}{\varepsilon} f_{|i}. \tag{1}$$

3.1.2. *Undeformed and deformed configurations.* Let $\boldsymbol{b}_k$ denote the unit vector tangent to x_k for the undeformed configuration. Note $\boldsymbol{b}_i$ chosen this way are functions of x_k only. For example, for beam-like structures, we choose $\boldsymbol{b}_1$ to be tangent to the beam reference line x_1, and $\boldsymbol{b}_2$, $\boldsymbol{b}_3$ as unit vectors tangent to the cross-sectional coordinates x_α. As shown in Figure 8, we can describe the position of any material point of the original structure by its position vector $\boldsymbol{r}$ relative to a point O fixed in an inertial frame such

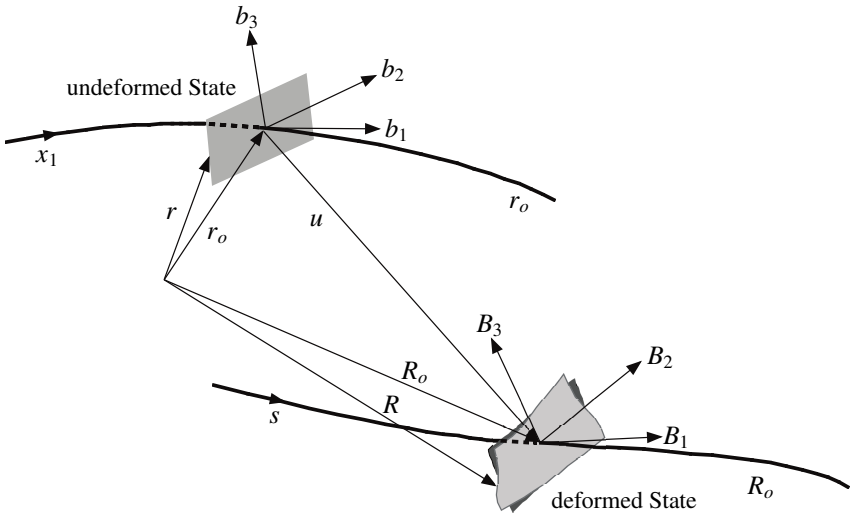

Figure 8. Deformation of a typical beam structure.

that

$$\boldsymbol{r}(x_k, y_\alpha) = \boldsymbol{r}_o(x_k) + \varepsilon y_\alpha \boldsymbol{b}_\alpha(x_k), \tag{2}$$

where $\boldsymbol{r}_o$ is the position vector from O to a material point of the macroscopic structural model. Note here x_k denotes only those coordinates remaining in the macroscopic structural model, and y_α corresponds to eliminated coordinates x_α. Because x_k is an arc-length coordinate, we have $\boldsymbol{b}_k = \partial \boldsymbol{r}_o / \partial x_k$.

When the original structure deforms, the particle that had position vector $\boldsymbol{r}$ in the undeformed configuration now has position vector $\boldsymbol{R}$ in the deformed configuration, such that

$$\boldsymbol{R}(x_k, y_j) = \boldsymbol{R}_o(x_k) + \varepsilon y_\alpha \boldsymbol{B}_\alpha(x_k) + \varepsilon w_i(x_k, y_j)\boldsymbol{B}_i(x_k), \tag{3}$$

where $\boldsymbol{R}_o$ denotes the position vector of the deformed structural model, $\boldsymbol{B}_i$ forms a new orthonormal triad for the deformed configuration, and εw_i are fluctuating functions introduced to accommodate all possible deformations other than those described by $\boldsymbol{R}_o$ and $\boldsymbol{B}_i$. $\boldsymbol{B}_i$ can be related with $\boldsymbol{b}_i$ through a direction cosine matrix, $C_{ij} = \boldsymbol{B}_i \cdot \boldsymbol{b}_j$, subject to the requirement that these two triads are the same in the undeformed configuration. $\boldsymbol{R}$ is expressed in terms of $\boldsymbol{R}_o$, $\boldsymbol{B}_i$, and w_i in (3), resulting in six times redundancy. Six constraints are needed to ensure a unique mapping. These constraints can be directly related with how we define $\boldsymbol{R}_o$ and $\boldsymbol{B}_i$ in terms of $\boldsymbol{R}$. For example, it is natural for us to define

$$\boldsymbol{R}_o = \langle\langle \boldsymbol{R} \rangle\rangle - \langle\langle \varepsilon y_\alpha \rangle\rangle \boldsymbol{B}_\alpha(x_k), \tag{4}$$

where $\langle\langle \cdot \rangle\rangle$ indicates averaging over the SG. If y_α is chosen such that $\langle\langle \varepsilon y_\alpha \rangle\rangle = 0$, $\boldsymbol{R}_o$ is defined as the average of the position vector of the original structure. Then (3) implies the following constraint on the fluctuating functions:

$$\langle\langle w_i \rangle\rangle = 0. \tag{5}$$

Note that for 3D structures y_α disappears and no requirement for $\langle\langle \varepsilon y_\alpha \rangle\rangle = 0$ is needed but the constraint in (5) remains.

The other three constraints can be used to specify $\boldsymbol{B}_i$. For plate/shell-like structures, we can select $\boldsymbol{B}_3$ in such a way that

$$\boldsymbol{B}_3 \cdot \boldsymbol{R}_{o,1} = 0, \quad \boldsymbol{B}_3 \cdot \boldsymbol{R}_{o,2} = 0, \tag{6}$$

which provides two constraints implying that we choose $\boldsymbol{B}_3$ normal to the reference surface of the deformed plate/shell. It should be noted that this choice has nothing to do with the well-known Kirchhoff hypothesis. In the Kirchhoff assumption, the transverse normal can only rotate rigidly without any local deformation. However, in the present formulation, we allow all possible deformations, classifying all deformations other than those described by $\boldsymbol{R}_o$ and $\boldsymbol{B}_i$ in terms of the fluctuating function $w_i \boldsymbol{B}_i$. The last constraint can be specified by the rotation of $\boldsymbol{B}_\alpha$ around $\boldsymbol{B}_3$ such that

$$\boldsymbol{B}_1 \cdot \boldsymbol{R}_{o,2} = \boldsymbol{B}_2 \cdot \boldsymbol{R}_{o,1}. \tag{7}$$

This constraint symmetrizes the macrostrains for a plate/shell model as defined in (19) later.

For beam-like structures, we can select $\boldsymbol{B}_\alpha$ in such a way that

$$\boldsymbol{B}_2 \cdot \boldsymbol{R}_{o,1} = 0, \quad \boldsymbol{B}_3 \cdot \boldsymbol{R}_{o,1} = 0, \tag{8}$$

which provides two constraints implying that we choose $\boldsymbol{B}_1$ to be tangent to the reference line of the deformed beam. Note that this choice is not the well-known Euler–Bernoulli assumption as the present formulation can describe all deformations of the cross-section. We can also prescribe the rotation of $\boldsymbol{B}_\alpha$ around $\boldsymbol{B}_1$ such that

$$\boldsymbol{B}_3 \cdot \frac{\partial \boldsymbol{R}}{\partial x_2} - \boldsymbol{B}_2 \cdot \frac{\partial \boldsymbol{R}}{\partial x_3} = 0, \tag{9}$$

which implies the following constraint on the fluctuating functions:

$$\langle\langle w_{2|3} - w_{3|2} \rangle\rangle = 0. \tag{10}$$

This constraint actually defines the twist angle of the macroscopic beam model in terms of the original position vector as pointed out in [Yu et al. 2012].

Thus the fluctuating functions are constrained according to (5). For beam structures, they are additionally constrained according to (10). Other constraints for the fluctuating functions can be introduced naturally into the formulation. For example, for periodic structures, fluctuating functions should be equal on periodic boundaries.

3.1.3. *Strain field.* If the local rotation (the rotation of a material point of the original structure subtracting the rotation needed for bringing $\boldsymbol{b}_i$ to $\boldsymbol{B}_i$) is small, it is convenient to use the Jauman–Biot–Cauchy strain according to the decomposition of the rotation tensor [Danielson and Hodges 1987]

$$\Gamma_{ij} = 1/2(F_{ij} + F_{ji}) - \delta_{ij}, \tag{11}$$

where δ_{ij} is the Kronecker symbol and F_{ij} is the mixed-basis component of the deformation gradient tensor defined as

$$F_{ij} = \boldsymbol{B}_i \cdot \boldsymbol{G}_a \boldsymbol{g}^a \cdot \boldsymbol{b}_j = \boldsymbol{B}_i \cdot (\boldsymbol{G}_k \boldsymbol{g}^k + \boldsymbol{G}_\alpha \boldsymbol{g}^\alpha) \cdot \boldsymbol{b}_j. \tag{12}$$

Here $\boldsymbol{g}^a$ are the 3D contravariant base vectors of the undeformed configuration and $\boldsymbol{G}_a$ are the 3D covariant basis vectors of the deformed configuration.

The contravariant base vector $\boldsymbol{g}^a$ is defined as

$$\boldsymbol{g}^a = \frac{1}{2\sqrt{g}} e_{aij} \boldsymbol{g}_i \times \boldsymbol{g}_j, \tag{13}$$

with e_{aij} as the 3D permutation symbol and $\boldsymbol{g}_i$ as the covariant base vector of undeformed configuration and $g = \det(\boldsymbol{g}_i \cdot \boldsymbol{g}_j)$.

From the undeformed configuration in (2), corresponding to the remaining macrocoordinate x_k, we obtain the covariant base vector as

$$\boldsymbol{g}_k = \frac{\partial \boldsymbol{r}}{\partial x_k} = \boldsymbol{b}_k + \varepsilon y_\alpha \frac{\partial \boldsymbol{b}_\alpha}{\partial x_k} = \boldsymbol{b}_k + \varepsilon y_\alpha \boldsymbol{k}_k \times \boldsymbol{b}_\alpha = \boldsymbol{b}_k + e_{i\alpha j} \varepsilon y_\alpha k_{ki} \boldsymbol{b}_j. \tag{14}$$

Here $\boldsymbol{k}_k = k_{ki} \boldsymbol{b}_i$ is the initial curvature vector corresponding to the remaining macrocoordinate x_k. This definition is consistent with $k_{kl}^{2\mathrm{D}}$ for initial curvatures of shells in [Yu and Hodges 2004a], if we let

$$k_{kl}^{2\mathrm{D}} = \alpha_{lm} k_{km}, \quad k_{k3}^{2\mathrm{D}} = k_{k3}, \tag{15}$$

with α_{lm} as the 2D permutation symbol: $\alpha_{11} = \alpha_{22} = 0$, $\alpha_{12} = -\alpha_{21} = 1$.

From the undeformed configuration in (2), corresponding to the eliminated macrocoordinate x_α, we obtain the covariant base vector as

$$\boldsymbol{g}_\alpha = \frac{\partial \boldsymbol{r}}{x_\alpha} = \frac{\partial \varepsilon y_\alpha}{x_\alpha} \boldsymbol{b}_\alpha = \boldsymbol{b}_\alpha. \tag{16}$$

From the deformed configuration in (3), corresponding to the remaining macrocoordinate x_k, we obtain the covariant base vector $\boldsymbol{G}_k$ as

$$\boldsymbol{G}_k = \frac{\partial \boldsymbol{R}}{\partial x_k} = \frac{\partial \boldsymbol{R}_o}{\partial x_k} + \varepsilon y_\alpha \frac{\partial \boldsymbol{B}_\alpha}{\partial x_k} + \varepsilon \frac{\partial w_i}{\partial x_k} \boldsymbol{B}_i + \varepsilon w_i \frac{\partial \boldsymbol{B}_i}{\partial x_k}. \tag{17}$$

From the deformed configuration in (3), corresponding to the eliminated macrocoordinate x_α, we obtain the covariant base vector as

$$\boldsymbol{G}_\alpha = \frac{\partial \boldsymbol{R}}{\partial x_\alpha} = \frac{\partial (\varepsilon y_\beta)}{\partial x_\alpha} \boldsymbol{B}_\beta + \varepsilon \frac{\partial w_i}{\partial x_\alpha} \boldsymbol{B}_i = \boldsymbol{B}_\alpha + \frac{\partial w_i}{\partial y_\alpha} \boldsymbol{B}_i. \tag{18}$$

A proper definition of the generalized strain measures for the macroscopic structural model is needed for the purpose of formulating the macroscopic structural analysis in a geometrically exact fashion. Following [Yu et al. 2012; Yu and Hodges 2004a; Pietraszkiewicz and Eremeyev 2009b], we introduce the following definitions:

$$\begin{aligned} \epsilon_{kl} &= \boldsymbol{B}_l \cdot \frac{\partial \boldsymbol{R}_o}{\partial x_k} - \delta_{kl}, \\ \kappa_{ki} &= (1/2) e_{iaj} \boldsymbol{B}_j \cdot \frac{\partial \boldsymbol{B}_a}{\partial x_k} - k_{ki}, \end{aligned} \tag{19}$$

where ϵ_{kl} is the Lagrangian stretch tensor and κ_{ki} is the Lagrangian curvature strain tensor (or the so-called wryness tensor). This definition corresponds to the kinematics of a nonlinear Cosserat continuum [Cosserat and Cosserat 1909] which allows six degrees of freedom (three translations and three rotations) for each material point no matter whether the macroscopic structural model is 1D, 2D, or 3D. For beam-like structures, this definition reproduces the 1D generalized strain measures of the Timoshenko beam

model defined in [Hodges 2006]. If we restrict $\boldsymbol{B}_1$ to be tangent to $\boldsymbol{R}_o$, (8), this definition reproduces the 1D generalized strain measures of the Euler–Bernoulli beam model defined in the previous work. For plate/shell-like structures, if we use (7), we will have the symmetry $\epsilon_{12} = \epsilon_{21}$ as a constraint for the kinematics of the final plate/shell model. This definition reproduces the 2D generalized strain measures of the Reissner–Mindlin model defined in [Yu and Hodges 2004a]. If we further restrain $\boldsymbol{B}_3$ to be normal to the reference surface, (6), this definition reproduces the 2D generalized strain measures of the Kirchhoff–Love plate/shell model defined in [Yu et al. 2002]. For 3D structures, this definition corresponds to the natural strain measures defined in [Pietraszkiewicz and Eremeyev 2009b] for a nonlinear Cosserat continuum. Although the SG kinematics formulated this way has the potential to construct a Cosserat continuum model for the 3D macroscopic structural model even if the material of the original heterogeneous structure is described using a Cauchy continuum, we will restrict ourselves to the Cauchy continuum model for the 3D macroscopic structural model in this paper. In other words, we are seeking a symmetric Lagrangian stretch tensor ϵ_{kl} and negligible curvature strain tensor κ_{ki}. This can be achieved by constraining the global rotation needed for bringing $\boldsymbol{b_i}$ to $\boldsymbol{B_i}$ in a specific way, which can be illustrated more clearly using an invariant form of the definitions in (19). According to [Pietraszkiewicz and Eremeyev 2009a; 2009b], these definitions can be rewritten as

$$\begin{aligned} \epsilon &= \boldsymbol{C}^T \cdot \boldsymbol{F} - \boldsymbol{I}, \\ \kappa^T &= -(1/2)\boldsymbol{e} : \left(\boldsymbol{C}^T \cdot \frac{\partial \boldsymbol{C}}{\partial x_k} \boldsymbol{b}_k \right), \end{aligned} \tag{20}$$

where ϵ is the Lagrangian stretch tensor, κ the Lagrangian curvature strain tensor, $\boldsymbol{C} = \boldsymbol{B}_i \boldsymbol{b}_i$ is the global rotation tensor bringing $\boldsymbol{b}_i$ to $\boldsymbol{B}_i$, $\boldsymbol{F}$ is the deformation gradient tensor, $\boldsymbol{I} = \boldsymbol{b}_i \boldsymbol{b}_i$ is the second-order identity tensor, and $\boldsymbol{e} = -\boldsymbol{I} \times \boldsymbol{I}$ is the third-order skew Ricci tensor. If the global rotation tensor $\boldsymbol{C}$ is constrained to be decomposed from $\boldsymbol{F}$ according to the polar decomposition theorem,

$$\boldsymbol{F} = \boldsymbol{C} \cdot \boldsymbol{U}, \tag{21}$$

where $\boldsymbol{U}$ is a second-order positive symmetric tensor, then the definitions in (20) become

$$\begin{aligned} \epsilon &= \boldsymbol{C}^T \cdot (\boldsymbol{C} \cdot \boldsymbol{U}) - \boldsymbol{I} = \boldsymbol{U} - \boldsymbol{I}, \\ \kappa^T &= -(1/2)\boldsymbol{e} : \left(\boldsymbol{C}^T \cdot \frac{\partial \boldsymbol{C}}{\partial x_k} \boldsymbol{b}_k \right). \end{aligned} \tag{22}$$

Clearly, the Lagrangian stretch tensor ϵ becomes symmetric and is the definition of Jauman–Biot–Cauchy strain tensor. The Lagrangian curvature strain tensor κ corresponds to higher-order terms (gradient of the deformation gradient) which are commonly neglected in the Cauchy continuum model. This derivation is significant because it provides a geometrically exact description for the 3D solid and has demonstrated that the Cauchy continuum description can be actually reduced from the Cosserat continuum description. It is noted that restraining the global rotation tensor according to (21) is equivalent to introducing three constraints for $\boldsymbol{B}_i$ needed for 3D structures. With this derivation, the nonlinear kinematics of beams, plates/shells, and 3D structures can be described using a single, unified formulation.

To facilitate the derivation of the covariant vectors $\boldsymbol{G}_i$, we can rewrite the definitions in (19) as

$$\begin{aligned}\frac{\partial \boldsymbol{R}_o}{\partial x_k} &= \boldsymbol{B}_k + \epsilon_{kl}\boldsymbol{B}_l,\\ \frac{\partial \boldsymbol{B}_i}{\partial x_k} &= (\kappa_{kj} + k_{kj})\boldsymbol{B}_j \times \boldsymbol{B}_i.\end{aligned} \tag{23}$$

Note $\epsilon_{13} = \epsilon_{23} = 0$ for plate/shell-like structures due to (6) and $\epsilon_{12} = \epsilon_{13} = 0$ for beam-like structures due to (8).

Substituting (23) into (17), we can obtain more detailed expressions for the covariant base vectors of the deformed configuration $\boldsymbol{G}_k$ as follows:

$$\begin{aligned}\boldsymbol{G}_k &= \boldsymbol{B}_k + \epsilon_{kl}\boldsymbol{B}_l + \varepsilon y_\alpha \frac{\partial \boldsymbol{B}_\alpha}{\partial x_k} + \varepsilon \frac{\partial w_l}{\partial x_k}\boldsymbol{B}_l + \varepsilon \frac{\partial w_\alpha}{\partial x_k}\boldsymbol{B}_\alpha + \varepsilon w_l \frac{\partial \boldsymbol{B}_l}{\partial x_k} + \varepsilon w_\alpha \frac{\partial \boldsymbol{B}_\alpha}{\partial x_k}\\ &= \left(\delta_{kl} + \epsilon_{kl} + \varepsilon \frac{\partial w_l}{\partial x_k}\right)\boldsymbol{B}_l + \varepsilon(y_\alpha + w_\alpha)\frac{\partial \boldsymbol{B}_\alpha}{\partial x_k} + \varepsilon \frac{\partial w_\alpha}{\partial x_k}\boldsymbol{B}_\alpha + \varepsilon w_l \frac{\partial \boldsymbol{B}_l}{\partial x_k}\\ &= \left(\delta_{kl} + \epsilon_{kl} + \varepsilon \frac{\partial w_l}{\partial x_k}\right)\boldsymbol{B}_l + \varepsilon\left[e_{ij\alpha}(y_\alpha + w_\alpha)(\kappa_{kj} + k_{kj}) + \frac{\partial w_\alpha}{\partial x_k}\delta_{\alpha i} + e_{ijl}w_l(\kappa_{kj} + k_{kj})\right]\boldsymbol{B}_i.\end{aligned} \tag{24}$$

Using the expressions for $\boldsymbol{g}^a$ and $\boldsymbol{G}_a$, and dropping nonlinear terms due to the product of the curvature strains and the fluctuating functions, the 3D strain field defined in (11) can be written in the following matrix form:

$$\Gamma = \Gamma_h w + \Gamma_\epsilon \bar{\epsilon} + \varepsilon \Gamma_l w + \varepsilon \Gamma_R w, \tag{25}$$

where $\Gamma = \lfloor \Gamma_{11}\ \Gamma_{22}\ \Gamma_{33}\ 2\Gamma_{23}\ 2\Gamma_{13}\ 2\Gamma_{12} \rfloor^T$ denotes the strain field of the original structure, $w = \lfloor w_1\ w_2\ w_3 \rfloor^T$ the fluctuating functions, and $\bar{\epsilon}$ is a column matrix containing the generalized strain measures for the macroscopic structural model. For example, if the macroscopic structural model is a beam model, we have $\bar{\epsilon} = \lfloor \epsilon_{11}\ \kappa_{11}\ \kappa_{12}\ \kappa_{13} \rfloor^T$ with ϵ_{11} denoting the extensional strain, κ_{11} the twist, and κ_{12} and κ_{13} the bending curvatures. If the macroscopic structural model is a plate/shell model, we have $\bar{\epsilon} = \lfloor \epsilon_{11}\ \epsilon_{22}\ 2\epsilon_{12}\ \kappa_{11}^{2D}\ \kappa_{22}^{2D}\ \kappa_{12}^{2D} + \kappa_{21}^{2D} \rfloor^T$ with $\epsilon_{\alpha\beta}$ denoting the in-plane strains and $\kappa_{\alpha\beta}^{2D}$ denoting the curvature strains. If the macroscopic structural model is a 3D continuum model, we have $\bar{\epsilon} = \lfloor \epsilon_{11}\ \epsilon_{22}\ \epsilon_{33}\ 2\epsilon_{23}\ 2\epsilon_{13}\ 2\epsilon_{12} \rfloor^T$ with ϵ_{ij} denoting the Biot strain measures in a Cauchy continuum. Γ_h is an operator matrix which depends on the dimensionality of the SG. Γ_ϵ and Γ_l are two operator matrices, the form of which depends on the macroscopic structural model. Γ_R is an operator matrix existing only for those original structures featuring initial curvatures. The explicit expressions for these operators are given in the appendix for completeness.

3.2. ***Variational statement for SG.*** Although the SG concept can be used to analyze structures made of various types of materials, in this paper, we illustrate its use by focusing on structures made of elastic materials. These structures are governed by the variational statement

$$\delta U = \overline{\delta W}, \tag{26}$$

where δ is the usual Lagrangean variation, U is the strain energy, and $\overline{\delta W}$ is the virtual work of the applied loads. The over bar indicates that the virtual work needs not be the variation of a functional. For

a linear elastic material characterized using a 6×6 stiffness matrix D, the strain energy can be written as

$$U = \frac{1}{2} \int \frac{1}{\omega} \langle \Gamma^T D \Gamma \rangle \mathrm{d}\Omega, \tag{27}$$

where Ω is the volume of the domain spanned by x_k remaining in the macroscopic structural model. The notation $\langle \bullet \rangle = \int \bullet \sqrt{g} \mathrm{d}\omega$ is used to denote a weighted integration over the domain of the SG and ω denotes the volume of the domain spanned by y_k corresponding to the coordinates x_k remaining in the macroscopic structural model. If none of y_k is needed in the SG, then $\omega = 1$. For example, if a heterogeneous beam-like structure features a 3D SG, ω is the length of the SG in the y_1 direction, corresponding to x_1 remaining in the macroscopic beam model. If the heterogeneous beam-like structure features a 2D SG (uniform cross-section), y_1 is not needed for the SG and $\omega = 1$. ω for plate/shell-like structures or 3D structures can be obtained similarly.

For a Cauchy continuum, there may exist applied loads from tractions and body forces. The virtual work done by these applied loads can be calculated as

$$\overline{\delta W} = \int \frac{1}{\omega} \left(\langle \boldsymbol{p} \rangle \cdot \delta \boldsymbol{R} + \int_s \boldsymbol{Q} \cdot \delta \boldsymbol{R} \sqrt{c} \, \mathrm{d}s \right) \mathrm{d}\Omega, \tag{28}$$

where s denotes the boundary surfaces of the SG with applied traction force per unit area $\boldsymbol{Q} = Q_i \boldsymbol{B}_i$ and applied body force per unit volume $\boldsymbol{p} = p_i \boldsymbol{B}_i$. $\sqrt{c}$ is equal to 1 except for some degenerated cases where s is only a boundary curve of the SG and one of coordinates x_k is required to form the physical surfaces on which the load is applied. In this case, the differential area of the physical surface is equal to $\sqrt{c} \, \mathrm{d}s \mathrm{d}x_k$ with $\mathrm{d}s$ as the differential arc length along the boundary curve of SG. For example, for beam-like structures featuring a 2D SG, the SG boundary is the curve encircling the cross-section and $\sqrt{c} = \sqrt{g + (y_2(\mathrm{d}y_2/\mathrm{d}s) + y_3(\mathrm{d}y_3/\mathrm{d}s))^2 k_{11}^2}$.

Here $\delta \boldsymbol{R}$ is the Lagrangian variation of the displacement field in (3), such that

$$\delta \boldsymbol{R} = \overline{\delta q}_i \boldsymbol{B}_i + \varepsilon y_\alpha \delta \boldsymbol{B}_\alpha + \varepsilon \delta w_i \boldsymbol{B}_i + \varepsilon w_i \delta \boldsymbol{B}_i. \tag{29}$$

We may safely ignore products of the fluctuating functions and virtual rotations in $\delta \boldsymbol{R}$, because the fluctuating functions are small. The last term of the above equation is then dropped so that

$$\delta \boldsymbol{R} = \overline{\delta q}_i \boldsymbol{B}_i + \varepsilon y_\alpha \delta \boldsymbol{B}_\alpha + \varepsilon \delta w_i \boldsymbol{B}_i. \tag{30}$$

The virtual displacements and rotations of the macroscopic structural model are defined as

$$\overline{\delta q}_i = \delta \boldsymbol{R}_o \cdot \boldsymbol{B}_i, \quad \delta \boldsymbol{B}_\alpha = \overline{\delta \psi}_j \boldsymbol{B}_j \times \boldsymbol{B}_\alpha, \tag{31}$$

where $\overline{\delta q}_i$ and $\overline{\delta \psi}_i$ contain the components of the virtual displacement and rotation in the $\boldsymbol{B}_i$ system, respectively. They are functions of x_k only. Note $\overline{\delta \psi}_j$ are restrained to be derivable from $\overline{\delta q}_i$ and are higher-order terms that are neglected in a 3D structure described using the Cauchy continuum.

Then we can rewrite (30) as

$$\delta \boldsymbol{R} = \left(\overline{\delta q}_i + \varepsilon e_{j\alpha i} y_\alpha \overline{\delta \psi}_j + \varepsilon \delta w_i \right) \boldsymbol{B}_i. \tag{32}$$

Finally, we express the virtual work due to applied loads as

$$\overline{\delta W} = \overline{\delta W}_H + \varepsilon \, \overline{\delta W}^*, \tag{33}$$

where $\overline{\delta W}_H$ is the virtual work not related to the fluctuating functions w_i and $\overline{\delta W}^*$ is the virtual work related to the fluctuating functions. Specifically,

$$\overline{\delta W}_H = \int \left(f_i \overline{\delta q}_i + m_i \overline{\delta \psi}_i\right) \mathrm{d}\Omega, \quad \overline{\delta W}^* = \int \frac{1}{\omega}\left(\langle p_i \delta w_i\rangle + \oint Q_i \delta w_i \sqrt{c}\, \mathrm{d}s\right) \mathrm{d}\Omega, \tag{34}$$

with the generalized forces f_i and moments m_i defined as

$$f_i = \frac{1}{\omega}\left(\langle p_i\rangle + \int Q_i \sqrt{c}\, \mathrm{d}s\right), \quad m_i = \frac{e_{i\alpha j}}{\omega}\left(\langle \varepsilon y_\alpha p_j\rangle + \int \varepsilon y_\alpha Q_j \sqrt{c}\, \mathrm{d}s\right). \tag{35}$$

If we assume that p_i and Q_i are independent of the fluctuating functions, then we can rewrite $\overline{\delta W}^*$ as

$$\overline{\delta W}^* = \delta \int \frac{1}{\omega}\left(\langle p_i w_i\rangle + \int Q_i w_i \sqrt{c}\, \mathrm{d}s\right) \mathrm{d}\Omega. \tag{36}$$

In view of the strain energy in (27) and virtual work in (33) along with (34), the variational statement in (26) can be rewritten as

$$\int \frac{1}{\omega} \delta\left[\frac{1}{2}\langle \Gamma^T D \Gamma\rangle - \varepsilon\left(\langle p_i w_i\rangle + \int Q_i w_i \sqrt{c}\, \mathrm{d}s\right)\right] - \left(f_i \overline{\delta q}_i + m_i \overline{\delta \psi}_i\right) \mathrm{d}\Omega = 0. \tag{37}$$

If we attempt to solve this variational statement directly, we will encounter the same difficulty as in a direct analysis of the original structure. The main complexity comes from the fluctuating functions w_i, which are unknown functions of both micro- and macrocoordinates. To reduce the original continuum model to a macroscopic structural model, the common practice in structural modeling is to assume the fluctuating functions, *a priori*, in terms of some unknown functions (displacements, rotations, and/or strains) of x_k and some known functions of y_k. However, for arbitrary structures made with general composites, use of such *a priori* assumptions may introduce significant errors. Fortunately, the variational asymptotic method (VAM) [Berdichevsky 2009] provides a useful technique to obtain the fluctuating functions through an asymptotical analysis of the variational statement in (37). It does so in terms of the small parameter ε which is inherent in the composite structure to construct asymptotically correct macroscopic structural models. As the last two terms in (37) are not functions of w_i, we can conclude that the fluctuating function is governed by the following variational statement instead:

$$\delta\left[\frac{1}{2}\langle \Gamma^T D \Gamma\rangle - \varepsilon\left(\langle p_i w_i\rangle + \int Q_i w_i \sqrt{c}\, \mathrm{d}s\right)\right] = 0, \tag{38}$$

which can be considered as a variational statement for the SG as it is posed over the SG domain only. According to VAM, we can neglect the terms in the order of ε to construct the first approximation of the variational statement in (38) as

$$\delta(1/2)\langle(\Gamma_h w + \Gamma_\epsilon \bar{\epsilon})^T D(\Gamma_h w + \Gamma_\epsilon \bar{\epsilon})\rangle = 0. \tag{39}$$

It is noted here that only small geometry parameters are considered in this work. For structures made of materials featuring significantly different properties, small material parameters should also be introduced for the asymptotic analysis using VAM. It is also pointed out that VAM is used to discard energetically small terms which might cause difficulty in capturing some higher order local stresses. However, such

loss of information is mainly governed by the macroscopic structural model. In this work, only the classical structural models including the Euler–Bernoulli beam model, Kirchhoff–Love plate/shell model, and the Cauchy continuum model are constructed using MSG. It is our future plan to derive refined models such as the Reissner–Mindlin plate/shell model, Timoshenko beam model, and Cosserat continuum model using the unified MSG framework.

For very simple cases such as isotropic beams [Yu and Hodges 2004b], laminated plates [Yu 2005], and binary composites [Yu 2012], the variational statement in (39) can be solved exactly and analytically, while for general cases we need to turn to numerical techniques such as the finite element method for solutions. To this end, we need to express w using shape functions defined over SG as

$$w(x_k, y_j) = S(y_j)V(x_k). \tag{40}$$

Equation (40) is a standard way to solve (39) using the finite element method. Equation (39) is a variational statement used to solve for w given $\bar{\epsilon}$ with V as a function of x_k because of $\bar{\epsilon}$. Such a separation of variables is inherent in multiscale modeling and structural modeling approaches. S are the standard shape functions depending on the type of elements one uses, and can be found in typical finite element textbooks. V is what we need to solve for as the nodal values for the influence function based on the discretization.

Substituting (40) into (39), we obtain the following discretized version of the strain energy functional:

$$U = (1/2)(V^T E V + 2V^T D_{h\epsilon}\bar{\epsilon} + \bar{\epsilon}^T D_{\epsilon\epsilon}\bar{\epsilon}), \tag{41}$$

where

$$E = \langle(\Gamma_h S)^T D(\Gamma_h S)\rangle, \quad D_{h\epsilon} = \langle(\Gamma_h S)^T D\Gamma_\epsilon\rangle, \quad D_{\epsilon\epsilon} = \langle\Gamma_\epsilon^T D\Gamma_\epsilon\rangle. \tag{42}$$

Minimizing U in (41), subject to the constraints, gives us the linear system

$$EV = -D_{h\epsilon}\bar{\epsilon}. \tag{43}$$

It is clear that V linearly depends on $\bar{\epsilon}$, and the solution can be symbolically written as

$$V = V_0\bar{\epsilon}. \tag{44}$$

Substituting (44) back into (41), we can calculate the strain energy stored in the SG as the first approximation as

$$U = (1/2)\bar{\epsilon}^T(V_0^T D_{h\epsilon} + D_{\epsilon\epsilon})\bar{\epsilon} \equiv (\omega/2)\bar{\epsilon}^T\bar{D}\bar{\epsilon}, \tag{45}$$

where $\bar{D}$ is the effective stiffness to be used in the macroscopic structural model. For the Euler–Bernoulli beam model, $\bar{D}$ could be a fully populated 4×4 stiffness matrix; for the Kirchhoff–Love plate/shell model and Cauchy continuum model, $\bar{D}$ could be a fully populated 6×6 stiffness matrix.

Substituting the solved strain energy stored in the SG into (37), we can rewrite the variational statement governing the original structure as

$$\int\left[\delta(1/2)\bar{\epsilon}^T\bar{D}\bar{\epsilon} - f_i\overline{\delta q}_i - m_i\overline{\delta\psi}_i\right]\mathrm{d}\Omega = 0. \tag{46}$$

This variational statement governs the macroscopic structural model as it involves only fields which are unknown functions of the macrocoordinates x_k. The first term is the variation of the strain energy of

the macroscopic structural model and the rest of the terms are the virtual work done by generalized forces and moments. This variational statement governs the linear elastic behavior of structural elements (3D solid elements, 2D plate/shell elements, 1D beam elements) implemented in most commercial FEA software packages.

Often, we are also interested in computing the local fields within the original structure. With $\bar{\epsilon}$ obtained from the macroscopic structural analysis, the fluctuating function can be obtained as

$$w = SV_0\bar{\epsilon}. \tag{47}$$

The local displacement field can be obtained as

$$u_i = \bar{u}_i + x_\alpha(C_{\alpha i} - \delta_{\alpha i}) + \varepsilon w_j C_{ji}, \tag{48}$$

where u_i is the local displacement and $\bar{u}_i$ is the macroscopic displacement. For SGs having coordinates y_k with corresponding x_k existing in the macroscopic structural model, $\bar{u}_i$ should be interpreted as

$$\bar{u}_i = \bar{u}_i(x_{k_0}) + x_k\bar{u}_{i,k}, \tag{49}$$

where x_{k_0} is the center of the SG and $\bar{u}_{i,k}$ is the gradient along x_k evaluated at x_{k_0}.

The local strain field can be obtained as

$$\Gamma = (\Gamma_h SV_0 + \Gamma_\epsilon)\bar{\epsilon}. \tag{50}$$

The local stress field can be obtained directly using the Hooke's law as

$$\sigma = D\Gamma. \tag{51}$$

4. An analytical example: deriving the Kirchhoff–Love model for composite laminates

MSG presented above is very general so that it can handle a geometrically exact analysis for all types of structures with arbitrary heterogeneity. For the sake of simplicity, the above formulation will be specialized to derive the linear elastic Kirchhoff–Love model for composite laminates.

If we assume that the composite laminate is made of anisotropic homogeneous layers, the linear elastic behavior is governed by 3D elasticity in terms of 3D displacements u_i, strains ε_{ij}, and stresses σ_{ij}. To construct a plate model, we need to first express the 3D displacements in terms of 2D plate displacements:

$$\begin{aligned} u_1(x_1, x_2, y_3) &= \bar{u}_1(x_1, x_2) - y_3\bar{u}_{3,1} + w_1(x_1, x_2, y_3) \\ u_2(x_1, x_2, y_3) &= \bar{u}_2(x_1, x_2) - y_3\bar{u}_{3,2} + w_2(x_1, x_2, y_3) \\ u_3(x_1, x_2, y_3) &= \bar{u}_3(x_1, x_2) + w_3(x_1, x_2, y_3) \end{aligned} \tag{52}$$

Here $u_i(x_1, x_2, y_3)$ are 3D displacements, while $\bar{u}_i(x_1, x_2)$ are plate displacements which are functions of x_1, x_2 only. We also introduce 3D unknown fluctuating functions $w_i(x_1, x_2, y_3)$ to describe the information of 3D displacements which cannot be described by the simpler Kirchhoff–Love plate kinematics. Note that the displacement expressions in (52) have nothing to do with the celebrated Kirchhoff–Love assumptions. It can be considered as a change of variables to express the 3D displacements in terms of the displacement variables of the Kirchhoff–Love plate model and fluctuating functions. The Kirchhoff–Love assumptions are equivalent to assuming $w_i = 0$. Since we consider that the original 3D model is

our true model, we construct the plate model as an approximation to the true model. To this end, we need to define the plate displacements in terms of 3D displacements. A natural choice is

$$h\bar{u}_3(x_1, x_2) = \langle u_3 \rangle, \quad h\bar{u}_\alpha(x_1, x_2) = \langle u_\alpha(x_1, x_2, y_3) \rangle + \langle y_3 \rangle \bar{u}_{3,\alpha}, \tag{53}$$

which implies the following constraint on the fluctuating functions:

$$\langle w_i \rangle = 0. \tag{54}$$

Note if the origin of the thickness coordinate is at the middle of the plate thickness, (53) actually defines the plate displacements to be the average of the 3D displacements.

Then the 3D strain field can be obtained as

$$\begin{aligned}
\Gamma_{11} &= \epsilon_{11} + x_3\kappa_{11} + w_{1,1}, \\
2\Gamma_{12} &= 2\epsilon_{12} + 2x_3\kappa_{12} + w_{1,2} + w_{2,1}, \\
\Gamma_{22} &= \epsilon_{22} + x_3\kappa_{22} + w_{2,2}, \\
2\Gamma_{13} &= w_{1,3} + w_{3,1}, \\
2\Gamma_{23} &= w_{2,3} + w_{3,2}, \\
\Gamma_{33} &= w_{3,3},
\end{aligned}$$

with the linear plate strains defined as

$$\epsilon_{\alpha\beta}(x_1, x_2) = \tfrac{1}{2}(\bar{u}_{\alpha,\beta} + \bar{u}_{\beta,\alpha}), \quad \kappa^{2\mathrm{D}}_{\alpha\beta}(x_1, x_2) = -\bar{u}_{3,\alpha\beta}. \tag{55}$$

Here α, β denote subscript 1 or 2.

The 3D strain field can also be written in the following matrix form:

$$\varepsilon_e = \epsilon + x_3\kappa + I_\alpha w_{\|,\alpha}, \quad 2\varepsilon_s = {w_\|}' + e_\alpha w_{3,\alpha}, \quad \varepsilon_t = {w_3}', \tag{56}$$

with

$$\begin{aligned}
\varepsilon_e &= \lfloor \Gamma_{11} \;\; \Gamma_{22} \;\; 2\Gamma_{12} \rfloor^T, \\
2\varepsilon_s &= \lfloor 2\Gamma_{13} \;\; 2\Gamma_{23} \rfloor^T, \\
\varepsilon_t &= \Gamma_{33}, \\
\epsilon &= \lfloor \epsilon_{11} \;\; \epsilon_{22} \;\; 2\epsilon_{12} \rfloor^T, \\
\kappa &= \lfloor \kappa^{2\mathrm{D}}_{11} \;\; \kappa^{2\mathrm{D}}_{22} \;\; \kappa^{2\mathrm{D}}_{12} + \kappa^{2\mathrm{D}}_{21} \rfloor^T,
\end{aligned}$$

and

$$I_1 = \begin{bmatrix} 1 & 0 \\ 0 & 1 \\ 0 & 0 \end{bmatrix}, \quad I_2 = \begin{bmatrix} 0 & 0 \\ 1 & 0 \\ 0 & 1 \end{bmatrix}, \quad e_1 = \begin{Bmatrix} 1 \\ 0 \end{Bmatrix}, \quad e_2 = \begin{Bmatrix} 0 \\ 1 \end{Bmatrix}. \tag{57}$$

The strain energy can be used as a natural measure for information governing the linear elastic behavior. Twice of the strain energy can be written as

$$2U = \left\langle \begin{Bmatrix} \varepsilon_e \\ 2\varepsilon_s \\ \varepsilon_t \end{Bmatrix}^{\mathrm{T}} \begin{bmatrix} C_e & C_{es} & C_{et} \\ C_{es}^{\mathrm{T}} & C_s & C_{st} \\ C_{et}^{\mathrm{T}} & C_{st}^{\mathrm{T}} & C_t \end{bmatrix} \begin{Bmatrix} \varepsilon_e \\ 2\varepsilon_s \\ \varepsilon_t \end{Bmatrix} \right\rangle. \tag{58}$$

The explicit expression after dropping smaller energy contributions due to $w_{i,\alpha}$ according to VAM is

$$2U_0 = \langle (\epsilon + x_3\kappa)^{\mathrm{T}} C_e (\epsilon + x_3\kappa) + w_\parallel'^{\mathrm{T}} C_s w_\parallel' + w_3'^{\mathrm{T}} C_t w_3' + 2(\epsilon + x_3\kappa)^{\mathrm{T}} C_{es} w_\parallel' + 2(\epsilon + x_3\kappa)^{\mathrm{T}} C_{et} w_3' + 2 w_\parallel'^{\mathrm{T}} C_{st} w_3' \rangle. \quad (59)$$

Minimizing this energy with respect to the fluctuating function w_i along with the constraints in (54), we reach the following Euler–Lagrange equations:

$$((\epsilon + x_3\kappa)^{\mathrm{T}} C_{es} + w_\parallel{}'^{\mathrm{T}} C_s + w_3{}' C_{st}^{\mathrm{T}})' = \lambda_\parallel, \quad (60)$$

$$((\epsilon + x_3\kappa)^{\mathrm{T}} C_{et} + w_\parallel{}'^{\mathrm{T}} C_{st} + w_3{}' C_t)' = \lambda_3, \quad (61)$$

where $\lambda_\parallel = \lfloor \lambda_1 \lambda_2 \rfloor^T$ and λ_3 denote the Lagrange multipliers enforcing the constraints in (54). The boundary conditions on the top and bottom surfaces are

$$(\epsilon + x_3\kappa)^{\mathrm{T}} C_{es} + w_\parallel{}'^{\mathrm{T}} C_s + w_3{}' C_{st}^{\mathrm{T}} = 0, \quad (62)$$

$$(\epsilon + x_3\kappa)^{\mathrm{T}} C_{et} + w_\parallel{}'^{\mathrm{T}} C_{st} + w_3{}' C_t = 0. \quad (63)$$

We can conclude that the above two equations should be satisfied at every point through the thickness and solve for $w_\parallel{}'^{\mathrm{T}}$ and $w_3{}'$ as

$$w_\parallel{}'^{\mathrm{T}} = -(\epsilon + x_3\kappa) C_{es}^* C_s^{-1}, \quad (64)$$

$$w_3{}' = -(\epsilon + x_3\kappa) C_{et}^* C_t^{*-1}, \quad (65)$$

with

$$C_t^* = C_t - C_{st}^{\mathrm{T}} C_s^{-1} C_{st}, \quad C_{et}^* = C_{et} - C_{es} C_s^{-1} C_{st}, \quad C_{es}^* = C_{es} - C_{et}^* C_{st}^{\mathrm{T}} / C_t^*. \quad (66)$$

w_i can be solved by simply integrating through the thickness along with the interlaminar continuity.

Substituting the solved fluctuating functions into (59), we have

$$2U_0 = \langle (\epsilon + x_3\kappa)^{\mathrm{T}} C_e^* (\epsilon + x_3\kappa) \rangle = \begin{Bmatrix} \epsilon \\ \kappa \end{Bmatrix}^{\mathrm{T}} \begin{bmatrix} A & B \\ B & D \end{bmatrix} \begin{Bmatrix} \epsilon \\ \kappa \end{Bmatrix}, \quad (67)$$

with

$$C_e^* = C_e - C_{es}^* C_s^{-1} C_{es}^{\mathrm{T}} - C_{et}^* C_{et}^{\mathrm{T}} / C_t^*, \quad A = \langle C_e^* \rangle, \quad B = \langle x_3 C_e^* \rangle, \quad D = \langle x_3^2 C_e^* \rangle. \quad (68)$$

This strain energy along with the work done by applied loads can be used to solve the 2D plate problem to obtain $\bar{u}_i, \epsilon, \kappa$. 3D displacements can be obtained after we have solved for w_i:

$$\begin{aligned} u_1(x_1, x_2, x_3) &= \bar{u}_1(x_1, x_2) - x_3 \bar{u}_{3,1} + w_1(x_1, x_2, y_3), \\ u_2(x_1, x_2, x_3) &= \bar{u}_2(x_1, x_2) - x_3 \bar{u}_{3,2} + w_2(x_1, x_2, y_3), \\ u_3(x_1, x_2, x_3) &= \bar{u}_3(x_1, x_2) + w_3(x_1, x_2, y_3). \end{aligned} \quad (69)$$

It is clear that the transverse normal does not remain rigid and normal according to Kirchhoff–Love assumptions in CLPT. Instead, the transverse normal can be deformed according to w_i.

3D strains can be obtained after neglecting the higher order terms $w_{i,\alpha}$, which are not contributing to the approximation of the plate energy. That is,

$$\varepsilon_e = \epsilon + x_3\kappa, \quad 2\varepsilon_s = -(\epsilon + x_3\kappa) C_{es}^* C_s^{-1}, \quad \varepsilon_{33} = -(\epsilon + x_3\kappa) C_{et}^* C_t^{*-1}. \quad (70)$$

Clearly, the strain field is not in-plane as what is traditionally assumed using Kirchhoff–Love assumptions in CLPT. Instead, transverse shear and normal strains both could exist.

By directly using the above strain field along with the Hooke's law in the original 3D elasticity theory, 3D stresses can be obtained as

$$\sigma_e = C_e^*(\epsilon + x_3\kappa,) \quad \sigma_s = 0, \quad \sigma_{33} = 0 \tag{71}$$

It can be observed that the Kirchhoff–Love model derived using MSG satisfies the plane-stress assumption invoked in CLPT. However, this is not assumed *a priori* but derived by using MSG.

5. Numerical examples

The MSG developed in this paper was implemented into a computer code called SwiftComp. A few examples are used here to demonstrate the application and validity of MSG and its companion code SwiftComp. It can be theoretically shown that one can specialize MSG to reproduce the well established theory of composite beams known as Variational Asymptotic Beam Sectional analysis (VABS) [Cesnik and Hodges 1997; Yu et al. 2012], the theory of composite plates/shells known as Variational Asymptotic Plate And Shell analysis (VAPAS) [Yu 2005] and the micromechanics theories known as Variational Asymptotic Method for Unit Cell Homogenization (VAMUCH) [Yu and Tang 2007] and theories of heterogeneous plates and beams [Lee and Yu 2011a; 2011b]. We have verified that the current version of SwiftComp can reproduce all the results of VAMUCH, and the classical models of VABS and VAPAS. Particularly, an extensively benchmark study for micromechanics theories and codes has been recently carried out by cdmHUB (Composites Design and Manufacturing HUB) and the results have shown that MSG and SwiftComp can achieve the versatility and accuracy of 3D FEA with much less computational time, which clearly demonstrates the advantage of MSG in micromechanics. Interested readers are directed to the report and database of the Micromechanics Simulation Challenge available at https://cdmhub.org/projects/mmsimulationchalleng. Here, a few examples which cannot be handled by current versions of VAMUCH, VABS, and VAPAS are used to demonstrate the application of MSG and SwiftComp.

5.1. ***A cross-ply laminate.*** First, we will use a simple cross-ply laminate example to demonstrate the application of MSG. As shown in Figure 9, a four-layer cross-ply [90°/0°/90°/0°] laminate with length

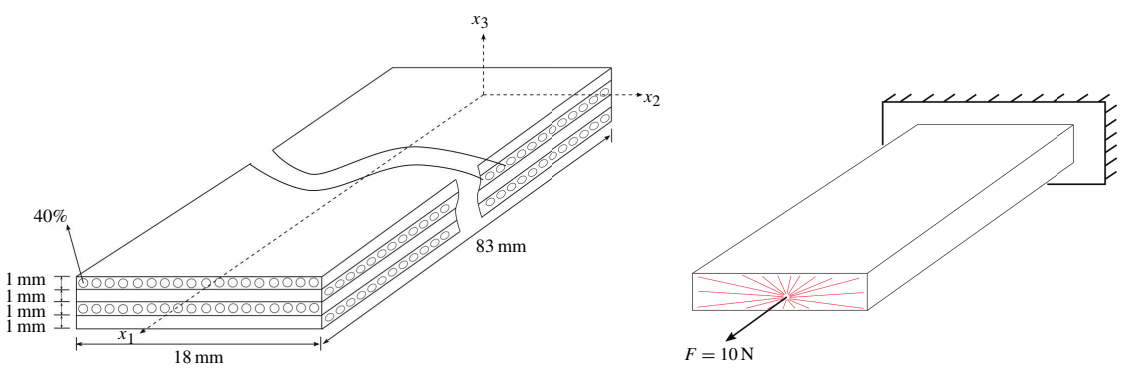

Figure 9. Sketch of the four-layer cross-ply laminate.

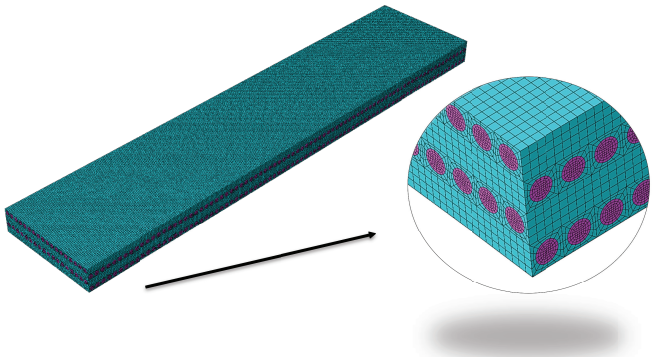

Figure 10. 3D finite element mesh of the four-layer cross-ply laminate.

83 mm, width 18 mm, and height 4 mm is clamped at one end and loaded at the other end with a 10 N tensile force at the center of the cross-section. The composite prepreg is assumed to have square packing with 40% fiber volume fraction. The fiber and matrix are assumed to be isotropic, with a Young's modulus of 276 GPa and a Poisson's ratio of 0.28 for the fiber and a Young's modulus of 4.76 GPa and a Poisson's ratio of 0.37 for the matrix.

It is noted here that this example is not representative of a typical fiber reinforced composite laminate, as usually each layer could contain many more fibers instead of one fiber per layer thickness as assumed here for simplicity. The purpose of this example is not to question CLPT's modeling capability for conventional laminates, which could be the subject of a future publication. Instead, this example is used to demonstrate the accuracy and efficiency of alternative analysis options provided by MSG. There are two common approaches to analyze this type of structure: 3D FEA using solid elements to mesh all of the microstructural details (see Figure 10) and lamination theory with lamina constants computed by a micromechanics approach (see Figure 2). Using 3D FEA, the laminate is meshed with 2,294,784 C3D20R elements with a total of 9,319,562 nodes in ABAQUS to achieve a fair convergence of stress predictions. Using MSG, we can also analyze the structure as a plate with the constitutive relations provided through an analysis of the corresponding SG as shown in Figure 11, where the SG is meshed in ABAQUS using 1,536 20-noded brick elements with 7,585 total nodes, and the reference surface is meshed with 2,988 STRI3 elements containing 1,596 nodes. Because the length is much larger than both the height and width, the structure can also be analyzed as a beam with the constitutive relations provided

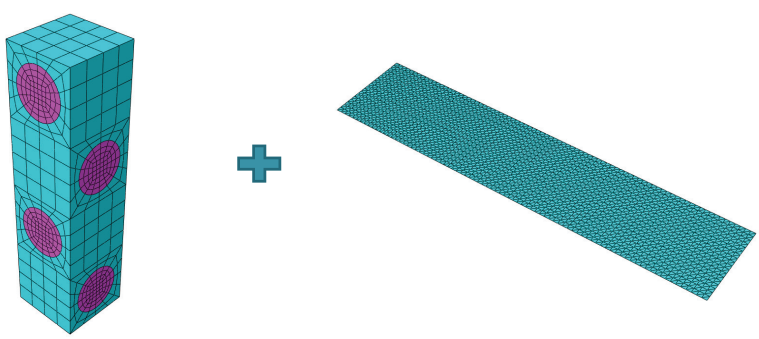

Figure 11. SwiftComp-based plate analysis.

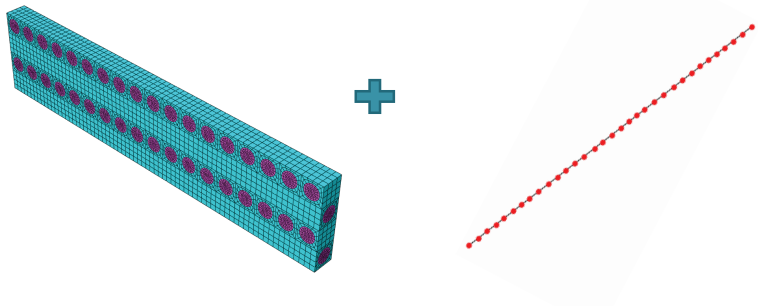

Figure 12. SwiftComp-based beam analysis.

through an analysis of the corresponding SG as shown in Figure 12. The SG is meshed with 27,648 20-noded brick elements with 124,409 nodes total, and the reference line is meshed with 83 two-noded line elements with 84 nodes total.

Different analysis approaches require different computing resources and time. Using 3D FEA, we used a computer with 48 cores and it took ABAQUS 7 days 11 hours and 37 minutes to finish the analysis. For the lamination theory, we used the composite layup analysis in ABAQUS with the same surface mesh as shown in Figure 11. To compute the lamina constants, SwiftComp only requires a 2D SG which is much more efficient than other computational homogenization approaches which usually require a 3D domain to obtain the complete set of properties [Fish 2013]. The micromechanics analysis and the laminate analysis are finished within 30 seconds. For SwiftComp-based plate analysis, homogenization of the SG to compute the plate stiffness takes 6 seconds, the surface analysis takes 28 seconds, and dehomogenization to obtain 3D local fields takes 6 seconds. For SwiftComp-based beam analysis, homogenization of SG to compute the beam stiffness takes 3 minutes and 14 seconds, the beam analysis takes 0.02 second, and dehomogenization to obtain 3D local fields takes 1 minute 21 seconds. Except for the 3D FEA, all the other analyses were done in the same computer using only 1 core. The other analyses are several orders of magnitude more efficient than 3D FEA. SwiftComp adds small overhead for the constitutive modeling including both the homogenization and dehomogenization processes in comparison to the traditional lamination theory for this simple static analysis. However, constitutive modeling is usually done once, while many global structural analyses using beam elements or plate elements are needed in the real design and analysis of composite structures. In other words, the small overhead added by SwiftComp could be negligible for most cases.

Different analysis approaches result in different predictions. The displacements at the center of the loaded tip are shown in Table 1. SwiftComp-based plate and beam analyses achieve excellent agreement

Analysis methods	Deflection (mm)	Extension (mm)
3D FEA	$2.7124{\cdot}10^{-3}$	$2.0849{\cdot}10^{-4}$
SwiftComp beam analysis	$2.7146{\cdot}10^{-3}$	$2.0873{\cdot}10^{-4}$
SwiftComp plate analysis	$2.7084{\cdot}10^{-3}$	$2.0832{\cdot}10^{-4}$
ABAQUS Composite layup	$2.5264{\cdot}10^{-3}$	$2.0804{\cdot}10^{-4}$

Table 1. Displacements predicted by different analyses.

with 3D FEA. Lamination theory using ABAQUS layup analysis provides an excellent prediction for the minor displacement (extension), but introduces about 7% error for the major displacement (deflection) in comparison to 3D FEA. The prediction of the detailed stress distribution within composites is also very important, as these quantities could be directly related with the failure of the structure. Consider the stress distribution through the thickness at $x_1 = 41.5\,\text{mm}$, $x_2 = 0.5\,\text{mm}$. Note at this point x_3 is passing through the diameter of one of the fibers. As shown in Figures 13, 14, and 15, both SwiftComp-based plate analysis and beam analysis achieve excellent agreement with 3D FEA for all the nontrivial stress components while the ABAQUS composite layup analysis shows significant discrepancies from 3D FEA. It is clear that the composite layup analysis predicts stress discontinuities happening at the wrong locations and the maximum stresses predicted by the composite layup analysis are also very different from 3D FEA. The composite layup analysis cannot predict the transverse normal stress (σ_{33}) due to its inherent plane-stress assumption, while SwiftComp-based plate and beam analyses still remain in very good agreement with 3D FEA, although the magnitude is small compared to the other two in-plane stress components. It can be observed that for this problem, SwiftComp can achieve similar accuracy as 3D FEA but with orders of magnitude savings in computing time and resources. Regarding the relatively larger discrepancy between SwiftComp and 3D FEA for σ_{33}, it is mainly because we could not further refine the 3D FEA model due to the limitation of the workstation we can access (56 CPUs with 256 GB RAM). We have verified that for simpler cases such as a two-layer plate of the same example, we can get a perfect match with 3D FEA. We have done mesh convergence studies for many problems and MSG consistently converges faster than 3D FEA due to the semianalytical nature of MSG.

5.2. ***Sandwich beam with periodically varying cross-sections.*** The next example is used to demonstrate the application of MSG to analyze beams with spanwise heterogeneities which can be commonly found in civil engineering applications. It is a sandwich beam with periodically variable cross-section studied

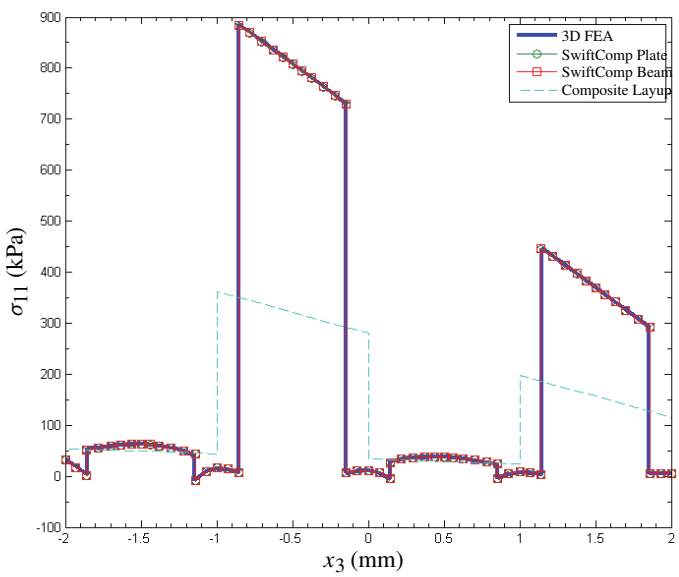

Figure 13. σ_{11} distribution through the thickness ($x_1 = 41.5\,\text{mm}$, $x_2 = 0.5\,\text{mm}$).

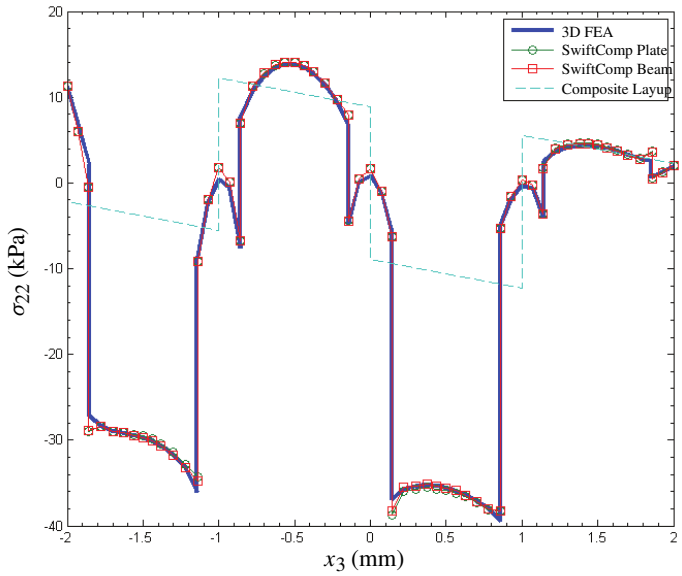

Figure 14. σ_{22} distribution through the thickness ($x_1 = 41.5$ mm, $x_2 = 0.5$ mm).

in [Dai and Zhang 2008]. The geometric parameters for each configuration are given in Figure 16. Note that although all the SGs in Figure 16 are uniform along y_2, the SG must be 3D because they are used to form a beam structure and y_2 is one of the cross-sectional coordinates (Figure 17). All sandwich beams in the above cases have the same core material properties (material indicated by blue color in the figure) of $E_c = 3.5$ GPa, $\nu_c = 0.34$ and face sheet material properties (indicated by purple color in the figure) of $E_f = 70$ GPa, $\nu_c = 0.34$. Also note that although these beams are studied in [Dai and Zhang 2008],

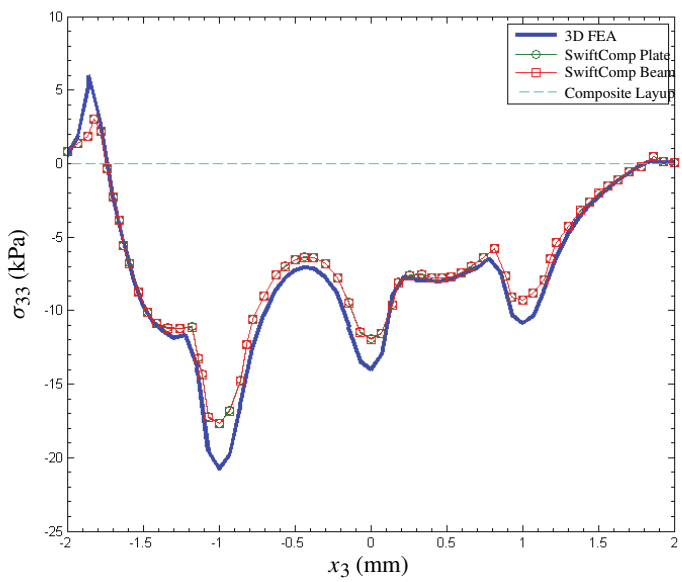

Figure 15. σ_{33} distribution through the thickness ($x_1 = 41.5$ mm, $x_2 = 0.5$ mm).

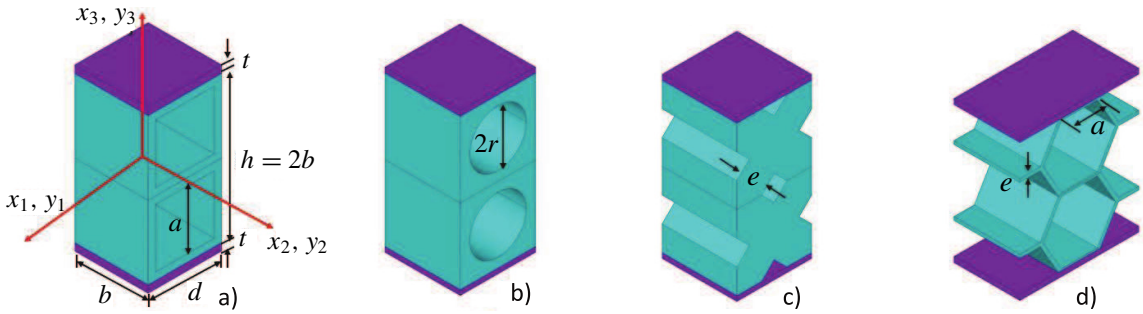

Figure 16. The structure genome for sandwich beams with different cross-sections: a) square holes ($b = d = 1.5$ m, $t = 0.1$ m, $a = 1$ m); b) circular holes ($b = d = 1.5$ m, $t = 0.1$ m, $r = 0.5614$ m); c) cross-shaped holes ($b = d = 1.5$ m, $t = 0.1$ m, $e = 0.7071$ m); d) hexagonal holes ($b = 1.23745$ m, $d = 2b$, $t = 0.1$ m, $a = 0.7887$ m, $e = 0.6431$ m).

	[Dai and Zhang 2008]	SwiftComp	NIAH
square holes	5.669	5.576	5.576
circular holes	5.176	5.537	5.554
cross-shaped holes	5.486	5.805	5.891
hexagonal holes	2.875	2.888	2.886

Table 2. Effective beam bending stiffness of sandwich beams predicted by different methods (all units are 10^{10} N·m^2).

only bending stiffnesses are given. In fact, the effective stiffness for the classical beam model in general should be represented by a fully populated 4×4 matrix. This example is also studied in [Yi et al. 2015] using a novel finite implementation of the asymptotic homogenization theory applied to beams. The effective bending stiffnesses predicted by the analytical formulas in [Dai and Zhang 2008], those of [Yi et al. 2015] denoted as NIAH standing for Novel Implementation of Asymptotic Homogenization, and SwiftComp are listed in Table 2. The details of these approaches can be found in the cited references.

As can be observed, SwiftComp predictions have an excellent agreement with NIAH and are slightly different from those in [Dai and Zhang 2008]. However, the present approach is more versatile than that in the previous work because that paper only provides analytic formulas for the bending stiffness of beams made of materials characterized only by one material constant, the Young's modulus, while SwiftComp can estimate all the engineering beam constants represented by a 4×4 stiffness matrix (possibly fully populated) for the most general anisotropic materials by factorizing the coefficient matrix in the linear system (Equation (43)) only once. NIAH results are obtained using multiple runs of a commercial finite element code, which requires much more computing time than SwiftComp.

5.3. ***Sandwich panel with a corrugated core.*** The last example is to demonstrate the application of MSG to model plates with in-plane heterogeneities. It is a corrugated-core sandwich panel, a concept used for Integrated Thermal Protection Systems (ITPS) studied in [Sharma et al. 2010]. The ITPS panel along with the details of the SG is sketched in Figure 18. Both materials are isotropic with $E_1 = 109.36$

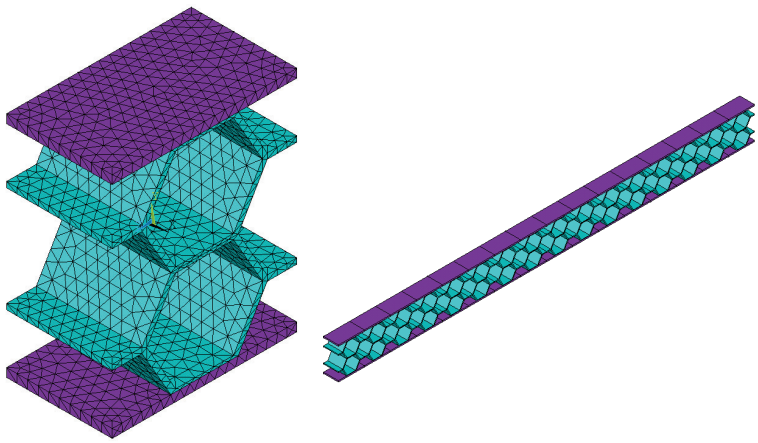

Figure 17. A sandwich beam with hexagonal holes.

GPa, $\nu_1 = 0.3$ for material 1, and $E_2 = 209.482$ GPa, $\nu_2 = 0.063$ for material 2. Although 3D unit cells are needed for the study in the previous reference, only a 2D SG is necessary for SwiftComp as it is uniform along one of the in-plane directions. The effective stiffness for the Kirchhoff–Love plate model can be represented using the A, B and D matrices known in CLPT. Results obtained in the previous reference are compared with SwiftComp in Tables 3, 4 and 5. SwiftComp predictions agree very well when compared to those results with the biggest difference (around 1%) appearing for the extension-bending coupling stiffness (B_{11}). However, the present approach is much more efficient because using the approach in [Sharma et al. 2010] one needs to carry out six analyses of a 3D unit cell under six different sets of boundary conditions and load conditions and postprocess the 3D stresses to compute the

	A_{11}	A_{12}	A_{22}	A_{33}
[Sharma et al. 2010]	2.83	0.18	2.33	1.07
SwiftComp	2.80	0.18	2.33	1.08

Table 3. Effective extension stiffness of ITPS (all units in 10^9 N/m).

	D_{11}	D_{12}	D_{22}	D_{33}
[Sharma et al. 2010]	3.06	0.22	2.85	1.32
SwiftComp	3.03	0.22	2.87	1.32

Table 4. Effective bending stiffness of ITPS (all units in 10^6 N·m).

	B_{11}	B_{13}	B_{22}	B_{33}
[Sharma et al. 2010]	−71.45	−3.36	−34.05	−71.45
SwiftComp	−70.67	−3.31	−34.06	−71.42

Table 5. Effective coupling stiffness of ITPS (all units in 10^6 N).

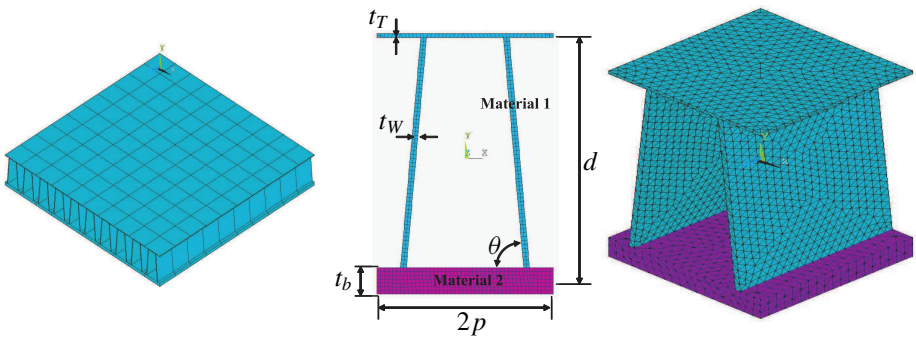

Figure 18. Sketch of the ITPS panel (left) and its SG ($t_T = 1.2\,\text{mm}$, $t_B = 7.49\,\text{mm}$, $t_W = 1.63\,\text{mm}$, $p = 25\,\text{mm}$, $d = 70\,\text{mm}$, and $\theta = 85°$).

plate stress resultants. Using the present approach, one only needs to carry out one analysis of a 2D SG without applying carefully crafted boundary conditions and postprocessing.

6. Conclusion

This paper developed a unified theory for multiscale constitutive modeling of composites based on the concept of SG. The SG facilitates a mathematical decoupling of the original complex analysis of composite structures into a constitutive modeling over the SG and a macroscopic structural analysis. The MSG presented in this paper enables a multiscale constitutive modeling approach with the following unique features:

- Use of SG to connect microstructures and macroscopic structural analyses. Intellectually, SG enables us to view constitutive modeling for structures as applications of micromechanics. Technically, SG empowers us to systematically model complex build-up structures with heterogeneities.
- Use of VAM to avoid *a priori* assumptions commonly invoked in other approaches, providing the rigor needed to construct mathematical models with excellent tradeoffs between efficiency and accuracy.
- Decouple the original problem into two sets of analyses: a constitutive modeling and a structural analysis. This allows the structural analysis to be formulated exactly as a general (1D, 2D, or 3D) continuum, the analysis of which is readily available in commercial FEA software packages. This also confines all approximations to the constitutive modeling, the accuracy of which is guaranteed to be the best by the VAM.

A general-purpose computer code, called SwiftComp, was developed to implement MSG along with several examples to demonstrate its application. This code can be used as a plug-in for commercial FEA software packages to accurately model structures made of anisotropic heterogeneous materials using traditional structural elements.

Although only theoretical details and implementation have been worked out for linear elastic behavior of periodic structures for which a SG can be easily identified, the basic framework is also applicable to nonlinear behavior of aperiodic heterogeneous structures, which are topics for future work.

Appendix

Γ_h is an operator matrix which depends on the dimensionality of the SG. If the SG is 3D, we have

$$\Gamma_h = \begin{bmatrix} 1/\sqrt{g_1}(\partial/\partial y_1) & 0 & 0 \\ 0 & 1/\sqrt{g_2}(\partial/\partial y_2) & 0 \\ 0 & 0 & (\partial/\partial y_3) \\ 0 & (\partial/\partial y_3) & 1/\sqrt{g_2}(\partial/\partial y_2) \\ (\partial/\partial y_3) & 0 & 1/\sqrt{g_1}(\partial/\partial y_1) \\ 1/\sqrt{g_2}(\partial/\partial y_2) & 1/\sqrt{g_1}(\partial/\partial y_1) & 0 \end{bmatrix}, \tag{72}$$

where $\sqrt{g_1} = \sqrt{g_2} = 1$ for plate-like structures or 3D structures; $\sqrt{g_1} = 1 - \varepsilon y_2 k_{13} + \varepsilon y_3 k_{12}$, $\sqrt{g_2} = 1$ for beam-like structures; and $\sqrt{g_1} = 1 + \varepsilon y_3 k_{12}$, $\sqrt{g_2} = 1 - \varepsilon y_3 k_{21}$ for shell-like structures.

If the SG is a lower-dimensional one, one just needs to vanish the corresponding term corresponding to the microcoordinates which are not used in describing the SG. For example, if the SG is 2D, we have

$$\Gamma_h = \begin{bmatrix} 0 & 0 & 0 \\ 0 & 1/\sqrt{g_2}(\partial/\partial y_2) & 0 \\ 0 & 0 & (\partial/\partial y_3) \\ 0 & (\partial/\partial y_3) & 1/\sqrt{g_2}(\partial/\partial y_2) \\ (\partial/\partial y_3) & 0 & 0 \\ 1/\sqrt{g_2}(\partial/\partial y_2) & 0 & 0 \end{bmatrix}. \tag{73}$$

If the SG is 1D, we have

$$\Gamma_h = \begin{bmatrix} 0 & 0 & 0 \\ 0 & 0 & 0 \\ 0 & 0 & (\partial/\partial y_3) \\ 0 & (\partial/\partial y_3) & 0 \\ (\partial/\partial y_3) & 0 & 0 \\ 0 & 0 & 0 \end{bmatrix}. \tag{74}$$

Γ_ϵ is an operator matrix, the form of which depends on the macroscopic structural model. If the macroscopic structural model is the 3D Cauchy continuum model, Γ_ϵ is the 6×6 identity matrix. If the macroscopic structural model is a beam model, we have

$$\Gamma_\epsilon = \frac{1}{\sqrt{g_1}} \begin{bmatrix} 1 & 0 & \varepsilon y_3 & -\varepsilon y_2 \\ 0 & 0 & 0 & 0 \\ 0 & 0 & 0 & 0 \\ 0 & 0 & 0 & 0 \\ 0 & \varepsilon y_2 & 0 & 0 \\ 0 & -\varepsilon y_3 & 0 & 0 \end{bmatrix}. \tag{75}$$

If the macroscopic structural model is a plate/shell model, we have

$$\Gamma_\epsilon = \begin{bmatrix} 1/\sqrt{g_1} & 0 & 0 & \varepsilon y_3/\sqrt{g_1} & 0 & 0 \\ 0 & 1/\sqrt{g_2} & 0 & 0 & \varepsilon y_3/\sqrt{g_2} & 0 \\ 0 & 0 & 0 & 0 & 0 & 0 \\ 0 & 0 & 0 & 0 & 0 & 0 \\ 0 & 0 & 0 & 0 & 0 & 0 \\ 0 & 0 & 1/2\left(\dfrac{1}{\sqrt{g_1}}+\dfrac{1}{\sqrt{g_2}}\right) & 0 & 0 & 1/2\left(\dfrac{\varepsilon y_3}{\sqrt{g_1}}+\dfrac{\varepsilon y_3}{\sqrt{g_2}}\right) \end{bmatrix}. \tag{76}$$

Note the above expression is obtained with the understanding that the difference between κ_{12} and κ_{21} is of higher order and negligible if we are not seeking a higher-order approximation of the initial curvatures.

Γ_l is an operator matrix, the form of which depends on the macroscopic structural model. If the macroscopic structural model is 3D, Γ_l has the same form as Γ_h in (72) with $\partial/\partial y_k$ replaced with $\partial/\partial x_k$, that is

$$\Gamma_l = \begin{bmatrix} 1/\sqrt{g_1}(\partial/\partial x_1) & 0 & 0 \\ 0 & 1/\sqrt{g_2}(\partial/\partial x_2) & 0 \\ 0 & 0 & (\partial/\partial x_3) \\ 0 & (\partial/\partial x_3) & 1/\sqrt{g_2}(\partial/\partial x_2) \\ (\partial/\partial x_3) & 0 & 1/\sqrt{g_1}(\partial/\partial x_1) \\ 1/\sqrt{g_2}(\partial/\partial x_2) & 1/\sqrt{g_1}(\partial/\partial x_1) & 0 \end{bmatrix}. \tag{77}$$

Of course for 3D structures, we have $\sqrt{g_1} = \sqrt{g_2} = 1$.

If the macroscopic structural model is a lower-dimensional one, one just needs to vanish the corresponding term corresponding to the macrocoordinates which are not used in describing the macroscopic structural model. For example, if the macroscopic structural model is a 2D plate/shell model, we have

$$\Gamma_l = \begin{bmatrix} 1/\sqrt{g_1}(\partial/\partial x_1) & 0 & 0 \\ 0 & 1/\sqrt{g_2}(\partial/\partial x_2) & 0 \\ 0 & 0 & 0 \\ 0 & 0 & 1/\sqrt{g_2}(\partial/\partial x_2) \\ 0 & 0 & 1/\sqrt{g_1}(\partial/\partial x_1) \\ 1/\sqrt{g_2}(\partial/\partial x_2) & 1/\sqrt{g_1}(\partial/\partial x_1) & 0 \end{bmatrix}. \tag{78}$$

If the macroscopic structural model is the 1D beam model, we have

$$\Gamma_l = \begin{bmatrix} 1/\sqrt{g_1}(\partial/\partial x_1) & 0 & 0 \\ 0 & 0 & 0 \\ 0 & 0 & 0 \\ 0 & 0 & 0 \\ 0 & 0 & 1/\sqrt{g_1}(\partial/\partial x_1) \\ 0 & 1/\sqrt{g_1}(\partial/\partial x_1) & 0 \end{bmatrix}. \tag{79}$$

Γ_R is an operator matrix existing only for those heterogeneous structures featuring initial curvatures. For prismatic beams, plates or 3D structures, Γ_R vanishes. For those structures having initial curvatures

such as initially twisted/curved beams or shells, the form of Γ_R depends on the macroscopic structural model. If the macroscopic structural model is a 1D beam model,

$$\Gamma_R = \frac{1}{\sqrt{g_1}} \begin{bmatrix} k_{11}\left(y_3\frac{\partial}{\partial y_2} - y_2\frac{\partial}{\partial y_3}\right) & -k_{13} & k_{12} \\ 0 & 0 & 0 \\ 0 & 0 & 0 \\ 0 & 0 & 0 \\ -k_{12} & k_{11} & k_{11}\left(y_3\frac{\partial}{\partial y_2} - y_2\frac{\partial}{\partial y_3}\right) \\ k_{13} & k_{11}\left(y_3\frac{\partial}{\partial y_2} - y_2\frac{\partial}{\partial y_3}\right) & -k_{11} \end{bmatrix}. \tag{80}$$

If the macroscopic structural model is a 2D shell model,

$$\Gamma_R = \begin{bmatrix} 0 & -k_{13}/\sqrt{g_1} & k_{12}/\sqrt{g_1} \\ k_{23}/\sqrt{g_2} & 0 & -k_{21}/\sqrt{g_2} \\ 0 & 0 & 0 \\ 0 & k_{21}/\sqrt{g_2} & 0 \\ -k_{12}/\sqrt{g_1} & 0 & 0 \\ k_{13}/\sqrt{g_1} & -k_{23}/\sqrt{g_2} & 0 \end{bmatrix}. \tag{81}$$

Acknowledgments

This research is supported, in part, by the Air Force Office of Scientific Research (Agreement No. FA9550-13-1-0148) and by the Army Vertical Lift Research Center of Excellence at Georgia Institute of Technology and its affiliated program through a subcontract at Purdue University (Agreement No. W911W6-11-2-0010). The views and conclusions contained herein are those of the author and should not be interpreted as necessarily representing the official policies or endorsement, either expressed or implied, of the sponsors. The US Government is authorized to reproduce and distribute reprints notwithstanding any copyright notation thereon. The author also greatly appreciates the help from his student Ning Liu for providing results for the example in Section 5.1.

References

[Aboudi 1982] J. Aboudi, "A continuum theory for fiber-reinforced elastic-viscoplastic composites", *Int. J. Eng. Sci.* **20**:5 (1982), 605–621.

[Aboudi 1989] J. Aboudi, "Micromechanical analysis of composites by the method of cells", *Appl. Mech. Rev.* **42**:7 (1989), 193–221.

[Aboudi et al. 2001] J. Aboudi, M. J. Pindera, and S. Arnold, "Linear thermoelastic higher-order theory for periodic multiphase materials", *J. Appl. Mech.* **68**:5 (2001), 697–707.

[Aboudi et al. 2012] J. Aboudi, S. Arnold, and B. Bednarcyk, *Micromechanics of composite materials: a generalized multiscale analysis approach*, Elsevier, Amsterdam, 2012.

[Bensoussan et al. 1978] A. Bensoussan, J.-L. Lions, and G. Papanicolaou, *Asymptotic analysis for periodic structures*, Studies in Mathematics and its Applications **5**, North-Holland, Amsterdam, 1978.

[Berdichevsky 2009] V. Berdichevsky, *Variational principles of continuum mechanics I: Fundamentals*, Springer, Berlin, 2009.

[Berger et al. 2006] H. Berger, S. Kari, U. Gabbert, R. Rodriguez-Ramos, J. Bravo-Castillero, R. Guinovart-Diaz, F. Sabina, and G. Maugin, "Unit cell models of piezoelectric fiber composites for numerical and analytical calculation of effective properties", *Smart Mater. Struct.* **15**:2 (2006), 451–458.

[Carrera 2003] E. Carrera, "Historical review of zig-zag theories for multilayered plates and shells", *Appl. Mech. Rev.* **56**:3 (2003), 287–308.

[Carrera et al. 2012] E. Carrera, M. Maiarú, and M. Petrolo, "Component-wise analysis of laminated anisotropic composites", *Int. J. Solids Struct.* **49**:13 (2012), 1839–1851.

[Carrera et al. 2014] E. Carrera, M. Cinefra, M. Petrolo, and E. Zappino, *Finite element analysis of structures through unified formulation*, Wiley, Hoboken, NJ, 2014.

[Cesnik and Hodges 1997] C. Cesnik and D. Hodges, "VABS: a new concept for composite rotor blade cross-sectional modeling", *J. Amer. Helicopter Soc.* **42**:1 (1997), 27–38.

[Cheng and Batra 2000] Z.-Q. Cheng and R. Batra, "Three-dimensional asymptotic analysis of multiple-electroded piezoelectric laminates", *AIAA Journal* **38**:2 (2000), 317–324.

[Collier et al. 2002] C. Collier, P. Yarrington, and B. V. West, "Composite, grid-stiffened panel design for post buckling using HyperSizer", in *Proceedings of the 43rd AIAA/ASME/ASCE/AHS/ASC Structures, Structural Dynamics and Materials Conference* (Denver, 2002), AIAA, 2002.

[Cosserat and Cosserat 1909] E. Cosserat and F. Cosserat, *Théorie des corps déformables*, Hermann, Paris, 1909.

[Dai and Zhang 2008] G. Dai and W. Zhang, "Size effects of basic cell in static analysis of sandwich beams", *Int. J. Solids Struct.* **45**:9 (2008), 2512–2533.

[Danielson and Hodges 1987] D. Danielson and D. Hodges, "Nonlinear beam kinematics by decomposition of the rotation tensor", *J. Appl. Mech.* **54** (1987), 258–262.

[Demasi and Yu 2012] L. Demasi and W. Yu, "Assess the accuracy of the variational asymptotic plate and shell analysis (VAPAS) using the generalized unified formulation (GUF)", *Mech. Adv. Mater. Struct.* **20**:3 (2012), 227–241.

[Fish 2013] J. Fish, *Practical multiscaling*, Wiley, Hoboken, NJ, 2013.

[Ghosh 2011] S. Ghosh, *Micromechanical analysis and multi-scale modeling using the Voronoi cell finite element method*, CRC Press, Boca Raton, FL, 2011.

[Guedes and Kikuchi 1990] J. M. Guedes and N. Kikuchi, "Preprocessing and postprocessing for materials based on the homogenization method with adaptive finite element methods", *Comput. Methods Appl. Mech. Engrg.* **83**:2 (1990), 143–198.

[Hashin and Shtrikman 1962] Z. Hashin and S. Shtrikman, "A variational approach to the theory of the elastic behaviour of polycrystals", *J. Mech. Phys. Solids* **10** (1962), 343–352.

[Hill 1952] R. Hill, "The elastic behaviour of a crystalline aggregate", *Proc. Phys. Soc. Sec. A* **65** (1952), 349–354.

[Hodges 2006] D. Hodges, *Nonlinear composite beam theory*, AIAA, Washington, DC, 2006.

[Icardi and Ferrero 2010] U. Icardi and L. Ferrero, "Layerwise zig-zag model with selective refinement across the thickness", *Int. J. Numer. Methods Eng.* **84**:9 (2010), 1085–1114.

[Kalamkarov and Kolpakov 2001] A. L. Kalamkarov and A. G. Kolpakov, "A new asymptotic model for a composite piezoelastic plate", *Int. J. Solids Struct.* **38**:34-35 (2001), 6027–6044.

[Kalamkarov et al. 2009] A. Kalamkarov, I. Andrianov, and V. Danishevs'kyy, "Asymptotic homogenization of composite materials and structures", *Appl. Mech. Rev.* **62**:3 (2009), 030802.

[Khandan et al. 2012] R. Khandan, S. Noroozi, P. Sewell, and J. Vinney, "The development of laminated composite plate theories: a review", *J. Mater. Sci.* **47**:16 (2012), 5901–5910.

[Kim 2009] J. Kim, "An asymptotic analysis of anisotropic heterogeneous plates with consideration of end effects", *J. Mech. Mater. Struct.* **4**:9 (2009), 1535–1553.

[Kollár and Springer 2009] L. P. Kollár and G. S. Springer, *Mechanics of composite structures*, Cambridge University Press, 2009.

[Lee and Yu 2011a] C.-Y. Lee and W. Yu, "Homogenization and dimensional reduction of composite plates with in-plane heterogeneity", *Int. J. Solids Struct.* **48**:10 (2011), 1474–1484.

[Lee and Yu 2011b] C.-Y. Lee and W. Yu, "Variational asymptotic modeling of composite beams with spanwise heterogeneity", *Comput. Struct.* **89**:15–16 (2011), 1503–1511.

[Li and Wang 2008] S. Li and G. Wang, *Introduction to micromechanics and nanomechanics*, World Scientific, Hackensack, NJ, 2008.

[Mantari et al. 2012] J. Mantari, A. Oktem, and C. G. Soares, "A new trigonometric shear deformation theory for isotropic, laminated composite and sandwich plates", *Int. J. Solids Struct.* **49**:1 (2012), 43–53.

[Maugin and Attou 1990] G. A. Maugin and D. Attou, "An asymptotic theory of thin piezoelectric plates", *Quart. J. Mech. Appl. Math.* **43**:3 (1990), 347–362.

[Michel et al. 1999] J. C. Michel, H. Moulinec, and P. Suquet, "Effective properties of composite materials with periodic microstructure: a computational approach", *Comput. Methods Appl. Mech. Engrg.* **172**:1-4 (1999), 109–143.

[Milton 2002] G. W. Milton, *The theory of composites*, Cambridge Monographs on Applied and Computational Mathematics **6**, Cambridge University Press, 2002.

[Mori and Tanaka 1973] T. Mori and K. Tanaka, "Average stress in matrix and average elastic energy of materials with misfitting inclusions", *Acta Metallurgica* **21**:5 (1973), 571–574.

[Murakami and Toledano 1990] H. Murakami and A. Toledano, "A higher-order mixture homogenization of bi-laminated composites", *J. Appl. Mech.* **57** (1990), 388–296.

[Nemat-Nasser and Hori 1998] S. Nemat-Nasser and M. Hori, *Micromechanics: overall properties of heterogeneous materials*, 2nd ed., North-Holland Series in Applied Mathematics and Mechanics **37**, North-Holland, Amsterdam, 1998.

[Pagano and Rybicki 1974] N. Pagano and E. Rybicki, "On the significance of effective modulus solutions for fibrous composites", *J. Compos. Mater.* **8**:3 (1974), 214–228.

[Paley and Aboudi 1992] M. Paley and J. Aboudi, "Micromechanical analysis of composites by the generalized cells model", *Mech. Mater.* **14**:2 (1992), 127–139.

[Pietraszkiewicz and Eremeyev 2009a] W. Pietraszkiewicz and V. Eremeyev, "On vectorially parameterized natural strain measures of the nonlinear Cosserat continuum", *Int. J. Solids Struct.* **46**:11-12 (2009), 2477–2480.

[Pietraszkiewicz and Eremeyev 2009b] W. Pietraszkiewicz and V. A. Eremeyev, "On natural strain measures of the non-linear micropolar continuum", *Int. J. Solids Struct.* **46**:3-4 (2009), 774–787.

[Plagianakos and Saravanos 2009] T. S. Plagianakos and D. A. Saravanos, "Higher-order layerwise laminate theory for the prediction of interlaminar shear stresses in thick composite and sandwich composite plates", *Compos. Struct.* **87**:1 (2009), 23–35.

[Reddy 1984] J. Reddy, "A simple higher-order theory for laminated composite plates", *J. Appl. Mech.* **51**:4 (1984), 745–752.

[Reddy 2004] J. N. Reddy, *Mechanics of laminated composite plates and shells: theory and analysis*, CRC Press, Boca Raton, FL, 2004.

[Reddy and Cheng 2001] J. Reddy and Z.-Q. Cheng, "Three-dimensional solutions of smart functionally graded plates", *J. Appl. Mech.* **68**:2 (2001), 234–241.

[Sharma et al. 2010] A. Sharma, B. V. Sankar, and R. Haftka, "Homogenization of plates with microstructure and application to corrugated core sandwich panels", in *Proceedings of the 51st AIAA/ASME/ASCE/AHS/ASC Structures, Structural Dynamics, and Materials Conference* (Orlando, 2010), AIAA, 2010.

[Skoptsov and Sheshenin 2011] K. A. Skoptsov and S. V. Sheshenin, "Asymptotic analysis of laminated plates and shallow shells", *Mech. Solids* **46**:1 (2011), 129–138.

[Sun and Vaidya 1996] C. Sun and R. Vaidya, "Prediction of composite properties from a representative volume element", *Compos. Sci. Technol.* **56**:2 (1996), 171 – 179.

[Torquato 2002] S. Torquato, *Random heterogeneous materials*, Interdisciplinary Applied Mathematics **16**, Springer, New York, 2002.

[Williams 2005] T. O. Williams, "A two-dimensional, higher-order, elasticity-based micromechanics model", *Int. J. Solids Struct.* **42**:3-4 (2005), 1009–1038.

[Xiaohui et al. 2011] R. Xiaohui, C. Wanji, and W. Zhen, "A new zig-zag theory and C^0 plate bending element for composite and sandwich plates", *Arch. Appl. Mech.* **81**:2 (2011), 185–197.

[Yi et al. 2015] S. Yi, L. Xu, G. Cheng, and Y. Cai, "FEM formulation of homogenization method for effective properties of periodic heterogeneous beam and size effect of basic cell in thickness direction", *Comput. Struct.* **156** (2015), 1–11.

[Yu 2005] W. Yu, "Mathematical construction of a Reissner–Mindlin plate theory for composite laminates", *Int. J. Solids Struct.* **42**:26 (2005), 6680–6699.

[Yu 2012] W. Yu, "An exact solution for micromechanical analysis of periodically layered composites", *Mech. Res. Commun.* **46** (2012), 71–75.

[Yu and Hodges 2004a] W. Yu and D. H. Hodges, "A geometrically nonlinear shear deformation theory for composite shells", *J. Appl. Mech.* **71**:1 (2004), 1–9.

[Yu and Hodges 2004b] W. Yu and D. H. Hodges, "Elasticity solutions versus asymptotic sectional analysis of homogeneous, isotropic, prismatic beams", *J. Appl. Mech.* **71**:1 (2004), 15–23.

[Yu and Tang 2007] W. Yu and T. Tang, "Variational asymptotic method for unit cell homogenization of periodically heterogeneous materials", *Int. J. Solids Structures* **44**:11-12 (2007), 3738–3755.

[Yu et al. 2002] W. Yu, D. H. Hodges, and V. V. Volovoi, "Asymptotic generalization of Reissner–Mindlin theory: accurate three-dimensional recovery for composite shells", *Comput. Methods Appl. Mech. Eng.* **191**:44 (2002), 5087–5109.

[Yu et al. 2012] W. Yu, D. H. Hodges, and J. C. Ho, "Variational asymptotic beam sectional analysis—an updated version", *Int. J. Eng. Sci.* **59** (2012), 40–64.

[Zhang and Oskay 2016] S. Zhang and C. Oskay, "Reduced order variational multiscale enrichment method for elasto-viscoplastic problems", *Comput. Methods Appl. Mech. Engrg.* **300** (2016), 199–224.

[Zhang and Yu 2014] L. Zhang and W. Yu, "A micromechanics approach to homogenizing elasto-viscoplastic heterogeneous materials", *Int. J. Solids Struct.* **51**:23–24 (2014), 3878–3888.

Received 25 Sep 2015. Revised 28 Apr 2016. Accepted 11 May 2016.

WENBIN YU: wenbinyu@purdue.edu
Purdue University, 704 W Stadium Ave., West Lafayette, IN 47907, United States

JOURNAL OF MECHANICS OF MATERIALS AND STRUCTURES

msp.org/jomms

Founded by Charles R. Steele and Marie-Louise Steele

Cover photo: Mando Gomez, www.mandolux.com

See msp.org/jomms for submission guidelines.

JoMMS (ISSN 1559-3959) at Mathematical Sciences Publishers, 798 Evans Hall #6840, c/o University of California, Berkeley, CA 94720-3840, is published in 10 issues a year. The subscription price for 2016 is US $575/year for the electronic version, and $735/year (+$60, if shipping outside the US) for print and electronic. Subscriptions, requests for back issues, and changes of address should be sent to MSP.

JoMMS peer-review and production is managed by EditFLOW® from Mathematical Sciences Publishers.

PUBLISHED BY

mathematical sciences publishers

nonprofit scientific publishing

http://msp.org/

Journal of Mechanics of Materials and Structures
Volume 11, No. 4 July 2016

What discrete model corresponds exactly to a gradient elasticity equation?
VASILY E. TARASOV 329

A refined 1D beam theory built on 3D Saint-Venant's solution to compute homogeneous and composite beams
RACHED EL FATMI 345

A unified theory for constitutive modeling of composites
WENBIN YU 379

Modeling and experimentation of a viscoelastic microvibration damper based on a chain network model
CHAO XU, ZHAO-DONG XU, TENG GE and YA-XIN LIAO 413

An anisotropic piezoelectric half-plane containing an elliptical hole or crack subjected to uniform in-plane electromechanical loading
MING DAI, PETER SCHIAVONE and CUN-FA GAO 433

On the causality of the Rayleigh wave
BARIŞ ERBAŞ and ONUR ŞAHIN 449

On the modeling of dissipative mechanisms in a ductile softening bar
JACINTO ULLOA, PATRICIO RODRÍGUEZ and ESTEBAN SAMANIEGO 463